NASA Technical Memorandum 4412

Controls-Structures Interaction Guest Investigator Program

Overview and Phase I Experimental Results and Future Plans

Rudeen Smith-Taylor and Sharon E. Tanner
Langley Research Center
Hampton, Virginia

National Aeronautics and Space Administration
Office of Management
Scientific and Technical Information Program
1993

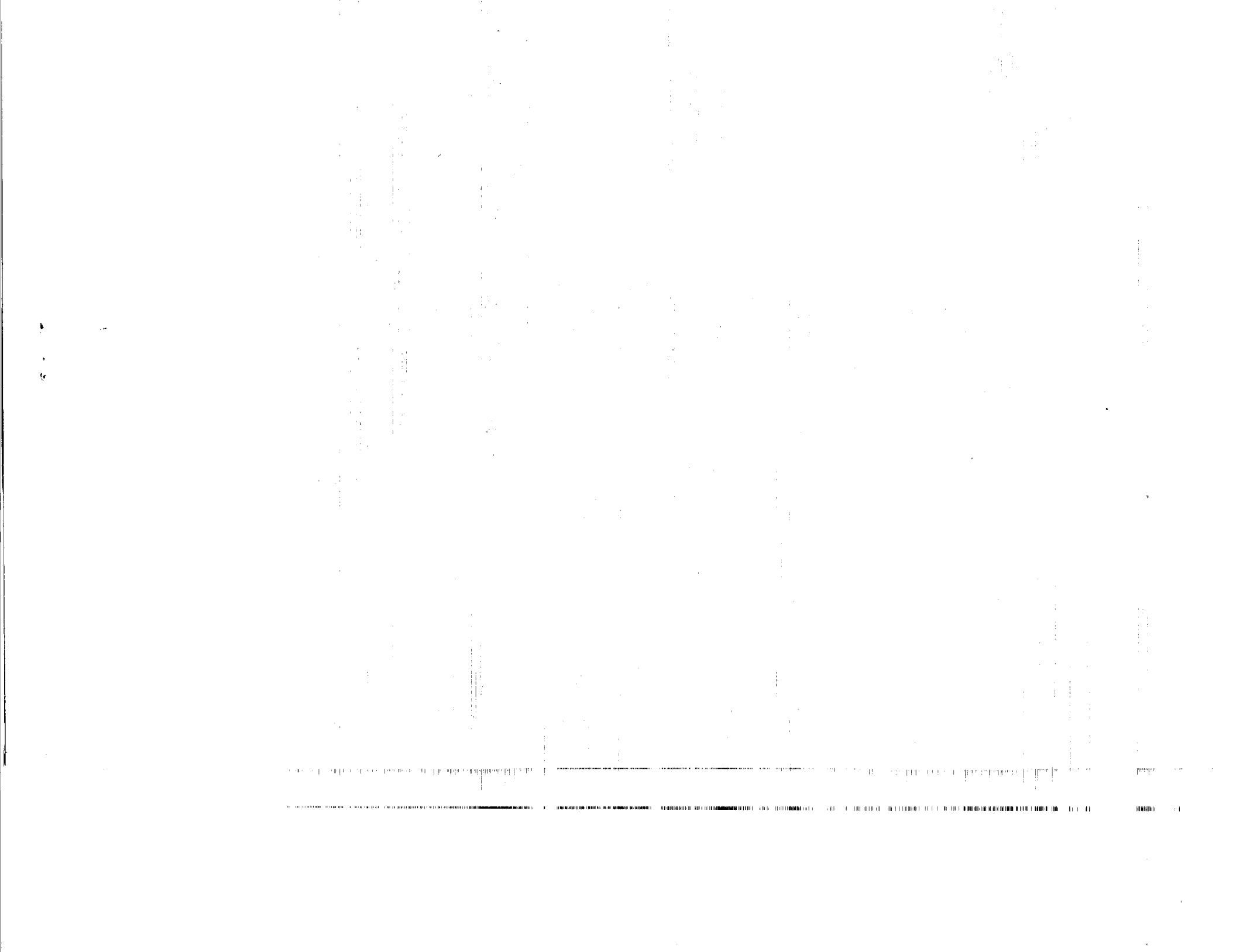

Nomenclature

ACES	Advanced Control Evaluation for Systems
AGS	advanced gimbal system
AMED	angular momentum exchange devices
ASTREX	Advanced Space Structures Technology Research Experiments
BET	base excitation table
BET-X	BET pulse disturbance
BGYRO-X	base rate gyro, X-axis
BGYRO-Y	base rate gyro, Y-axis
BGYRO-Z	base rate gyro, Z-axis
BLT	bi-linear thrusters
CAMAC	Computer Automated Measurement and Control
CASES	Controls, Astrophysics, and Structures Experiment in Space
CEM	CSI Evolutionary Model
CMG	control moment gyroscope
COFS	control of flexible structures
CSI	controls-structures interaction
DET-X	X-displacement optical detector
DET-Y	Y-displacement optical detector
DSPR	double-sensor parity relation
ERA	Eigensystem Realization Algorithm
FDI	failure detection and isolation
FRF	frequency response function
GI	guest investigator
IMC	image motion compensation
JPL	Jet Propulsion Laboratory
LaRC	Langley Research Center
LMED	linear momentum exchange device
LMED1-X	LMED 1, X-axis position command
LMED1-Y	LMED 1, Y-axis position command
LMED2-X	LMED 2, X-axis position command
LMED2-Y	LMED 2, Y-axis position command
LOS	line-of-sight
LQG	linear quadratic Gaussian
MCA	modal cost analysis
MEOP	maximum entropy/optimal projection
MFLOPS	million floating-point operations per second

MIMO	multiple-input–multiple-output
MPESS	Mission Peculiar Experiment Support Structure
MSFC	Marshall Space Flight Center
OAST	Office of Aeronautics and Space Technology
OPUS	optimal projection approach for uncertain systems
OVC	output variance constraint
QMC	Q-Markov covariance
RCS	reaction control system
SAFE	Solar Array Flight Experiment
SAPR	single-actuator parity relation
SISO	single-input–single-output
SSPR	single-sensor parity relation
TWA	torque-wheel actuators

Introduction

To integrate the stringent performance requirements with flexible space structures of the future, the control system designers must be aware of the structural dynamics of the spacecraft. Because of the uncertainties involved in controlling flexible structures, the design of these advanced control systems cannot rely solely on analytical development but requires experimental validation on dynamically realistic and structurally complex test facilities (ref. 1). This integrated approach, referred to as controls-structures interaction technology, is the focus of the NASA Controls-Structures Interaction (CSI) Program, which is managed by the Office of Aeronautics and Space Technology (OAST) at NASA Headquarters. The program is a multidisciplinary research activity whose objective is to develop and validate the technology needed for future spacecraft to meet increasingly demanding mission requirements. Three NASA centers, the Langley Research Center (LaRC), the Marshall Space Flight Center (MSFC), and the Jet Propulsion Laboratory (JPL), are cooperating to develop this technology.

The guest investigator (GI) program element of the CSI Program is the primary mechanism for evaluating and incorporating the ideas of industry and university researchers in the development of CSI technology. In phase I of the GI program, eight research teams from industry and academia participated in a 2-year research activity in which they used government ground test facilities to validate a broad range of CSI design techniques. Recently completed, this phase produced valuable results and increased appreciation for the need and difficulty of experimentally validating CSI research techniques and methodologies. This report includes a brief discussion of the CSI Program and a discussion of the GI program with emphasis on the test facilities, research methodologies, and experimental results of phase I.

The authors would like to express their appreciation to the Mini-MAST facility team at LaRC and the Advanced Control Evaluation for Systems (ACES) facility team at MSFC for hardware, software, and operational support during the 2-year GI program.

CSI Program

Future NASA space missions will require increased pointing precision, precise attitude control, and multiple-payload platforms with interacting control systems (ref. 2). The mission requirements will include control systems that are both highly integrated into and highly interactive with flexible structures. Experience shows that successful CSI system design requires a cooperative interdisciplinary trade-off between the control system and the structure dynamics throughout the design phase. Design methodologies and design-analysis tools must be developed that provide for these trade-off studies. Ground test methods must also be developed to support the verification of system performance of these integrated flexible structures and control techniques. To meet these technology goals, the CSI Program (1) develops and validates integrated design-analysis methods, (2) develops and demonstrates ground test methods to predict on-orbit performance, (3) obtains in-space experimental data to validate design-analysis and ground test methods, and (4) establishes design methods and criteria to qualify spacecraft for future space missions (ref. 2).

The five CSI Program elements addressing these issues are (1) configurations and concepts, (2) integrated analysis and design methods, (3) ground testing methods, (4) in-space flight experiments, and (5) a guest investigator program. The three NASA centers supporting the CSI Program, LaRC, MSFC, and JPL, have specific areas of expertise relating to these elements. LaRC emphasizes multiple-payload platforms and global control of large antennas. In addition, LaRC provides management for the technical CSI Program and the GI program. MSFC is concerned with flight qualification methods and ground tests, while JPL emphasizes development of design technology for optics-class applications and micro-precision-controlled structures.

Guest Investigator Program

The CSI guest investigator program objectives are (1) to solicit and support CSI research, (2) to provide advanced ground test facilities for experimental validation of this research, and (3) to make the experimental results available to the CSI community in a timely manner. The advancement of CSI technology greatly benefits from the participation of research experts from academia and industry. To obtain new and innovative research approaches, a general solicitation for participation in the GI program is made to the research community. The submitted proposals are reviewed and evaluated by an intercenter technical selection team or by a scientific peer review. The selections for award are based on technical merit, utilization of current government test facilities, and appropriate cost. The program is managed from LaRC by the CSI GI program manager, with technical monitors located at each test facility. Additional government and contractor personnel provide

Table 1. Phase I Guest Investigators

University or industry	Principal investigator	Research activity
Arizona State University	Bong Wie	Classical control theory with disturbance rejection
Boeing Aerospace Company	Michael Chapman	Nonlinear math modeling of strut compliance
California Institute of Technology	John Doyle and Gary Balas	H_∞ and μ-synthesis with uncertainties controller design
University of Cincinnati	Randall Allemang and Gary Slater	System identification and multivariable positivity control design
Dynamic Engineering, Inc.	Wilmer Reed	Passive and active suspension system design
Harris Corporation	David Hyland	Maximum entropy/optimal projection and decentralized hierarchical control
Massachusetts Institute of Technology	Wallace Vander Velde	System identification and fault detection and isolation methods
Purdue University	Robert Skelton	System identification using modal cost analysis and multivariable control design

the hardware, software, and operational support required to conduct the experiments at each of the ground test facilities.

Phase I began in February of 1988 with eight awards, five to universities and three to industry. The eight principal investigators and their primary research activities are shown in table 1. In addition, the appendix contains a list of these guest investigators and their addresses and telephone numbers as of November 1992.

Although the research activities differed greatly, each made significant contributions to the advancement of CSI technology. Two of the activities (Boeing Aerospace and Dynamic Engineering, Inc.) dealt with hardware modeling and design of suspension systems, respectively. The results of these two research activities are contained in references 3 and 4 and are not discussed in this report. The other six activities concentrated on system identification or the development and validation of active control techniques. The research goals of these six include application of specific control theories and failure detection methods. The research results are summarized after the descriptions of the two ground test facilities used during phase I: the Mini-MAST testbed at LaRC and the ACES testbed at MSFC.

CSI Ground Test Facilities

Mini-MAST Test Facility

The flexible-body component of the Mini-MAST facility was a 20-m-long deployable, retractable truss that was located at LaRC. (Since completion of phase I of the CSI guest investigator program, the facility has been dismantled and moved to the University of Colorado.) Manufactured by the Astro Aerospace Corporation using flight-quality materials, Mini-MAST was originally designed and built as a laboratory model of the 60-m MAST truss to be flown as part of the LaRC Control of Flexible Structures (COFS) Program, hence, the name Mini-MAST. This program was subsequently cancelled after the Mini-MAST structure had been built. Mini-MAST provided one of the first realistic testbeds for CSI technology research applicable to subcomponents that are expected to be used in future large space structures.

Figure 1 shows the Mini-MAST configuration used during phase I of the GI program. The truss,

weighing about 230 lb, was cantilevered vertically from a rigid foundation. The truss construction has three graphite/epoxy member types: longerons that run parallel to the beam axis, battens that form the triangular cross sections, and diagonals that lie in the beam face planes. The longerons and hinged diagonal members have pinned connections to titanium corner-body joints to allow for the necessary motion during deployment. The battens are rigidly connected to the corner bodies (ref. 5). The beam has 18 bays that deploy and retract, 2 bays at a time. During its use as a CSI testbed, Mini-MAST was locked in the fully deployed position. Clamps were added to ensure that the hinges did not open during testing.

Equipment mounting platforms were located at the tip (bay 18) and near the midpoint (bay 10). The three torque-wheel actuators (TWA's) mounted on the tip platform were the only actuators available for control. Each TWA weighed about 85 lb; thus, the fully equipped tip plate weighed about 364 lb. (The mid plate weighed about 109 lb.) The rated peak output of the TWA's was 50 ft-lb, a torque load that could break the cantilevered truss structure. The tip plate and mid plate held servo accelerometers for linear acceleration measurements and rate gyros for angular rate measurements. Noncontacting displacement sensors distributed along the beam axis were mounted alongside the truss for observing lateral displacement. The TWA's or three Unholtz-Dickie 50-lb shakers attached at bay 9 provided disturbance input to the structure.

The sensors, TWA's, and shakers were connected via fiber-optic cables to a real-time control computer that implemented control laws to actively damp the vibrational response of the structure. The mainframe computer, a Control Data Corporation CYBER 175 used for digital real-time controller implementation, can support sample data rates up to 200 Hz. Most research objectives on Mini-MAST, however, were accomplished with slower sample rates and greater control law computation time. For example, the computer had an 80-Hz update rate with a 40-state controller with 6 inputs and 3 outputs. The computer was interfaced to the testbed through the Computer Automated Measurement and Control (CAMAC) network, which supports data transmission at a rate of 50 megabits/sec.

The Mini-MAST truss had five structural modes below 10 Hz. The first two bending modes at about 0.86 Hz were followed by the first torsion mode at 4.2 Hz and a second pair of bending modes at about 6.1 Hz. There were 108 vibrational modes between the second bending modes at about 15 Hz and the second torsion mode at about 22.9 Hz. This cluster of modes was comprised primarily of the local bending modes of the diagonals and plate vibration modes of the equipment mounting platforms (ref. 6).

A finite-element model, updated to closely correlate with test data, was provided to each guest investigator. Modal models of the structure and an analytical model of all sensors and actuators were also provided for simulation and analysis of candidate control laws before facility testing. In addition, because the TWA's can cause structural damage to Mini-MAST under certain conditions, each controller was first run through a series of simulations by LaRC personnel to verify system stability and determine maximum member loads exerted on the truss elements during the closed-loop operation.

ACES Test Facility

The ACES ground test facility, located at MSFC, is a vertically suspended deployable beam, about 14 m long, supporting a 3-m offset antenna. Figure 2 shows the ACES configuration used during phase I. The Astromast beam, built by Astro Research as a flight backup for the Voyager magnetometer boom, is extremely lightweight ($\approx$5 lb), lightly damped (0.5–2 percent), and very flexible. It is symmetric and triangular in cross section with three continuous longerons forming the corners. The cross members divide the beam into 91 bays having equal length and mass and similar elastic properties. The beam exhibits a longitudinal twist of about 260° when fully deployed (ref. 7).

As shown in figure 2, the beam is suspended from an excitation table and attached to a payload mounting plate at the base. A two-axis advanced pointing gimbal system is also attached to the mounting plate. An antenna and two counter balance legs are appended to the beam tip, with pointing gimbal arms at the base, to form a configuration having modal characteristics of large space structures. The ACES configuration has 50 modes with frequencies under 15 Hz; the first torsion mode is at 0.05 Hz, and the first bending mode is at 0.14 Hz (ref. 8).

The hydraulically operated base excitation table (BET) provides disturbance inputs, and a three-axis gimbal system provides rotational control. The BET position is commanded with a programmable signal generator or a real-time computer system. The actuation system consists of one three-axis gimbal system, two two-axis momentum exchange systems, and one two-axis pointing system. The gimbal system is a two-axis advanced gimbal system (AGS), augmented with a third gimbal in the roll axis. Orthogonal pairs

of linear momentum exchange devices (LMED's) are located at two discrete locations along the length of the beam (ref. 9). The LMED's are proof-mass actuators that provide translational control forces. Through a collocated sensor-actuator pair, the LMED's apply a force and the sensors measure the resulting beam acceleration. Additionally, the measurement system has rate gyros and accelerometers mounted at the base and tip of the beam.

As shown in the numbered diagram in figure 2, an optical system, consisting of a fixed-position laser (no. 9), two mirrors (no. 8), and a two-axis detection plane (no. 7), provides a measure of control system performance. One of the optical system mirrors (no. 8) is mounted on a two-axis pointing gimbal system (no. 10) located on an extension arm appended to the base of the beam. This gimbaled mirror is used in a closed-loop image motion compensation (IMC) system composed of nos. 7–10 for the primary measurement of controller effectiveness. (See ref. 9.)

A finite-element model of the beam and a nonlinear simulation model were made available to each guest investigator for controller analysis before testing. Modeling showed the unsymmetrical ACES structure to be highly coupled with the beam, gimbals, LMED's, pointing gimbals, appendages, antenna, and counterweights. For example, several beam bending modes are coupled with localized antenna modes, pendulum modes, and appendage modes (ref. 9).

The hardware is supported by a real-time computer system that consists of a Hewlett-Packard 9000 computer interfaced with an Analogic Corporation array processor and a data acquisition system (COSMEC) built by MSFC. The system has a 50-Hz sample data rate and is equipped with 11 control actuators and 37 sensors that can accommodate a 50th-order controller. Unlike Mini-MAST, the ACES hardware and operating environment allowed the researchers to test new control laws without extensive simulation. This capability proved extremely important for validating integrated designs and for on-line tuning of closed-loop controllers.

Phase I Research Experiments and Results

Experimental results of the six guest investigator teams that performed research in the areas of system identification, fault detection, and controller development are discussed in this section. During the 2-year program, each guest investigator was required to perform validation testing at both the Mini-MAST and the ACES testbed previously described, while concentrating on a single testbed for a year. The research activities differed significantly in research objective and technical approach as well as in sensor and actuator selection. In the following sections, a general discussion of each research activity is followed by applications from each testbed and comments on the contributions each researcher made to the advancement of CSI technology.

Arizona State University

Bong Wie demonstrated the simplicity and effectiveness of applying classical control designs to the CSI testbeds. At both the Mini-MAST and the ACES testbed, various single-input–single-output (SISO) 2nd-order controllers were simultaneously applied to suppress the bending and torsional motion. Nonminimum phase compensation and periodic disturbance rejection were also demonstrated at both testbeds.

Nonminimum phase filtering was successfully used to add damping to secondary modes. By not restricting filter zeros to the left-half complex plane, these filters were shown to increase closed-loop damping of flexible modes while tolerating significant model uncertainty. The root locus method, Bode plots, and iterative refinement were the primary means used to develop robust compensators.

In the periodic disturbance rejection demonstration, an internal model for the disturbance (with known frequencies but unknown magnitudes and phases) was included as part of the compensator. The disturbance rejection filter was made of individual 4th-order filters, each designed for a specific frequency. The full filter then had as many pole-zero combinations, or dipoles, as frequencies in the periodic disturbance (ref. 10).

At Mini-MAST, both collocated and noncollocated SISO controllers were demonstrated with displacement measurements as feedback signals. Sensor output decoupling was required because the individual displacement sensors were not aligned with global axes and, therefore, were inherently coupled. Decoupled displacement measurements at bay 18 provided the Mini-MAST collocated feedback for the three torque-wheel actuators mounted on the bay 18 tip plate. The decoupled displacement measurements from bay 10 supplied feedback to the bay 18 actuators for the noncollocated controllers.

Figures 3 and 4 illustrate the success of applying these classical control concepts to the Mini-MAST testbed. Relative performance improvement is shown without specifying the magnitude of the results. In figure 3, the decoupled displacements and rotations

of the tip plate (bay 18) are shown for both the open-loop and the closed-loop system response with a collocated Mini-MAST controller. Active damping added to the first bending mode was 20 percent, as compared with 2 percent inherent damping. The closed-loop system response in the form of decoupled displacements and rotations of the mid plate is shown in figure 4 for a noncollocated controller with periodic disturbance rejection. The controller was turned on at Time = 0 sec, and a periodic disturbance was present from Time = 5 to 20 sec. Active damping was 15 percent for the first bending mode (ref. 10).

During the second year of the program, Wie applied the same classical control techniques to the ACES testbed; that is, he designed SISO controllers for single-axis control of the dominant loops that were identified the previous year by the Harris Corporation researchers. (These loops are subsequently discussed in the Harris section.) None of the ACES feedback signals used by Wie were collocated. Figure 5 shows an example of the experimental data from the ACES testbed. The open-loop time history is shown in figure 5(a) for the X-displacement optical detector (DET-X) to a pulse disturbance at the base excitation table (BET-X). As shown in figure 5(b), active damping was provided by simultaneously applying two classical SISO controllers in the AGS and IMC loops.

When a BET-X step function was used for excitation instead of the pulse function, the open-loop response was dominated by a 0.15-Hz mode, as shown in figure 6(a). This low-frequency mode was not adequately damped by the integrated AGS and IMC controllers, as shown in figure 6(b). However, including a dipole for disturbance rejection significantly improved the performance, as shown in figure 6(c). (See ref. 11.)

While modern control theory offers many promising results, as discussed in the following sections, the work of Wie demonstrated the potential for applying the simpler classical control theory to future space structures, especially when applied to persistent external periodic disturbances.

California Institute of Technology

John Doyle and Gary Balas used μ-analysis and μ-synthesis for their research effort. Control design using μ-synthesis is an iterative process that alternates between solving an optimal control problem with the H_∞ technique and a structured singular value (μ) analysis problem. Additive and multiplicative uncertainties were used to directly account for known and unknown errors such as structural modes eliminated from the reduced-order design models, unmodeled sensor and actuator dynamics, or inaccuracies in damping, frequencies, or mode shapes.

Doyle applied these techniques at the ACES testbed during the first year of the GI program. However, modeling difficulties created the need for excessively large uncertainty values, which in turn severely penalized controller performance. Even though these difficulties prevented any successful experimental tests at ACES, the experience proved useful in emphasizing the importance of accurate models (a problem faced with all model-based compensators).

During the second year, Balas successfully applied the same techniques to the Mini-MAST facility. Figure 7 shows the system block diagram incorporating both additive and multiplicative uncertainty descriptors. Initial controllers can be designed through use of such a system, with subsequent designs adding parametric uncertainties associated with variations in natural frequencies of the plant model.

To select feedback sensors, analytical studies were conducted with the assumption that no uncertainty existed in the system. Bay 18 accelerometers were found to be sufficient for observing and controlling the five modes below 10 Hz that dominated the Mini-MAST structural response. The performance objective selected for all controllers was the attenuation of truss displacement at bays 10 and 18. Additional analytical studies were performed to determine the most appropriate level of actuator input magnitude. Experimental validation later demonstrated the necessary trade-off between the levels allowed for actuator forces and rapidity of vibration suppression.

Eighteen controllers were designed, with varying actuator magnitude weights and uncertainty descriptors. Figure 8 shows results of one of the most aggressive controllers. (The drift in sensor output shown in this figure is attributable to wind loads on the tower to which the noncontacting displacement sensors were mounted.) Active damping of about 25 percent was added to the first bending motion of the truss, as shown in the tip-displacement sensors (fig. 8(a)). The second pair of bending modes was not attenuated as quickly, as shown in the displacement sensors at bay 10 (fig. 8(b)).

Finite-element models of Mini-MAST produced reasonably accurate structural response predictions for the testbed. Therefore, to experimentally test the ability of the μ-synthesis techniques to effectively handle modeling errors, Balas used modified and deliberately inaccurate natural frequencies to design a

set of controllers. Where the error added to the natural frequency was the maximum limit of the uncertainty, uncertainty levels of ±5, 11, and 20 percent were used randomly in either the positive or negative direction. Results from the controller designed with 20-percent uncertainty are shown in figure 9, where the active damping to the first bending motion was somewhat diminished.

Doyle and Balas demonstrated the success of μ-synthesis in handling certain types of modeling errors, specifically up to ±20-percent error in natural frequencies. However, their work highlighted the need for accurate models through the unsuccessful application of the techniques at the ACES facility. Also, the lack of robustness to parametric (structural) errors in the design model highlighted the need for system identification.

University of Cincinnati

The University of Cincinnati research effort was divided between two principal investigators. Randall Allemang led the effort to develop reliable state-space models, which Gary Slater was, in principle, to use for control law development.

In applying system identification techniques to actuator, structure, and sensor systems, Allemang highlighted the complexity that time delays add to the model. A number of single-reference and poly-reference time and frequency domain methods were used to estimate system parameters for the modal model.

Figure 10 shows the typical measured and synthesized frequency-response functions (FRF's) from the ACES testbed. Calculated residues for each system pole were used to estimate mode shapes and modal mass, which were then used to create the state-space models, with modal displacements and velocities as the states. The ACES work addressed nonlinearities, variations in system dynamics over time, and the lack of anti-aliasing protection. Significant variations in system behavior were noted in FRF's taken 3 months apart, as shown in the response of the same base gyro sensors (fig. 11.) Physical changes in the gyros were suspected because only FRF's involving those sensors were affected (ref. 12).

Two types of system nonlinearities were identified at the Mini-MAST testbed: nonlinear damping and an apparent nonlinear coupling between repeated modes. Nonlinear damping was an actual structural phenomenon, but nonlinear coupling was an error caused by measurement errors (leakage) and numerical conditioning of the multiple-input FRF algorithm in the presence of highly correlated input forces. This apparent coupling produced a phase gain at lightly damped resonances involving repeated roots, as shown in figure 12, at about 0.8 Hz and 6.2 Hz. Because the system is known to be causal but the data indicate noncausal characteristics, any model generated from this data cannot properly reflect the system's true structural characteristics.

In the control law development portion of the research effort, Slater chose the positive-real approach to controller design. This approach guarantees stability when the following three conditions are met: (1) sensors and actuators are ideal, (2) the system is continuous, and (3) the actuator and sensor pairs are collocated, act in the same direction, and are compatible (e.g., rate sensors paired with torque actuators or accelerometers paired with force actuators). Slater's work focused on applying positive-real controllers to actual, and therefore nonideal, hardware.

Scheduling delays at ACES resulted in Slater developing controllers based on a priori finite-element models provided by MSFC instead of using Allemang's state-space models. The AGS loop provided the most ideal test of a positivity design controller. However, effects of filters, actuator dynamics, and digital implementation invalidated the positivity approach. Persistent instabilities, even after positivity robustness conditions were added, led to the development of multivariable scaling and phase compensation techniques that resulted in stable closed-loop performance for an AGS-loop controller, as shown in figure 13. Subsequent to the completion of the GI program, Slater successfully applied a positivity-designed controller based on Allemang's identified state-space model, which was stable without the scaling and phase compensators. A discussion of this work was presented at the 8th VPISU Symposium on Dynamics and Control of Large Structures.

The multivariable scaling techniques for positivity-designed controllers hold promise for future large space structures because independent scale factors can be applied to all channels of the controller, including a zero scale factor. Thus, these factors can accommodate sensor or actuator failures without requiring controller redesign (ref. 13). This technique was successfully applied at ACES when one of the LMED's failed. With the use of a zero scale factor to remove a collocated sensor for the failed actuator, a multiple-input–multiple-output (MIMO) controller remained stable.

At Mini-MAST, Slater chose to use a high-fidelity finite-element model provided by LaRC for controller design. A number of positivity-designed SISO controllers were applied to the Z-axis torque-wheel ac-

tuator and rate gyro. Figure 14 shows open- and closed-loop results from one controller. A pseudo-positive-real approach produced relatively low-gain MIMO controllers that were applied to Mini-MAST, even though the system is not positive real. Successful application of the controllers to incompatible sensor and actuator pairs was demonstrated by limiting the bandwidth of the controller and the levels of the gain margin, as shown in figure 15. Figure 15(a) shows attenuation of tip displacements, and figure 15(b) shows increased oscillations in the second bending modes at bay 10. Instabilities resulted with higher gains.

The major contribution of Allemang's research was furthering system identification experiences with actuator-structure-sensor systems that are complicated by time delays, nonlinearities, and nonsymmetries. Slater's major contribution was the development of multivariable scaling and phase compensation techniques that can allow on-line controller tuning as well as tolerate sensor or actuator failures without controller redesign.

Harris Corporation

David Hyland led the Harris research team in the controller design application of the optimal projection approach for uncertain systems (OPUS). Hyland, assisted by Emmanuel Collins, Douglas Phillips, and James King, applied maximum entropy/optimal projection (MEOP) design, an OPUS process, in the design of their robust, high-performance controllers.

The Harris team emphasized controller simplification as essential in meeting stringent on-orbit processing limitations. Their MEOP design process is shown in figure 16. It begins with low- to moderate-authority controllers to which robustness is added through application of a homotopy algorithm, thus creating a maximum entropy design. (A homotopy is the continuous deformation of one function into another, a technique often used for the numerical solution of systems of nonlinear algebraic equations.) Next in the design process, the order of the controller is reduced through a balanced controller reduction; this step results in an approximation of a MEOP controller. Maximum entropy designs increase gain stability, allow order reduction in the controller bandwidth, and improve the controller's tolerance of uncertainties in damping, frequency, and location of system zeros. Optimal projection is a controller reduction methodology that uses the homotopy algorithm to solve coupled Riccati equations and Lyapunov equations; the result projects a large state-space controller onto a reduced space. The homotopy algorithm is then used to transform the approximation into a MEOP controller and, if necessary, used again to increase controller authority (ref. 14).

At Mini-MAST, the Harris researchers selected four accelerometers and a rate gyro as feedback sensors; they eliminated displacement sensors, which generally are not available in space. Their control objective for all controllers was to minimize the displacement at the tip of the Mini-MAST truss. Selecting the design model was the first crucial step in the controller design process. Harris researchers felt the Mini-MAST finite-element model predicted system responses with sufficient accuracy to be used as the design model.

Controllers with both decentralized and nearly centralized architectures were designed for the testbed. Each controller, including the nearly centralized controllers, contained one decentralized SISO constant-gain feedback loop from the torsional rate gyro to the corresponding (Z-axis) torque wheel to control the first torsional mode. This simple feedback loop provided more than 50-percent damping to the torsional mode, as shown in figure 17, which compares the closed-loop response of the torsional rate gyro with its open-loop response. (See ref. 14.)

A series of decentralized controllers combined the torsion loop controller with four other decentralized SISO controllers to increase the damping of the bending modes; each controller combination used a single accelerometer as feedback to one of the two remaining torque wheels. Thus, commands from two SISO controllers were summed, but with no cross-coupling terms, and then sent to a single actuator. The decentralized controller with the best performance was a 24th-order controller.

A series of nearly centralized controllers was also tested at Mini-MAST. This series combined the decentralized torsion loop controller with an additional feedback loop that coordinated the two torque wheels with feedback from the same accelerometers used in the decentralized architecture. The most effective nearly centralized controller was a 33rd-order controller.

Figure 18 compares the open-loop response of a Mini-MAST tip-displacement sensor to a single-pulse excitation (fig. 18(a)) with the closed-loop response with various controllers in the loop: a classically designed pseudo-rate feedback controller (fig. 18(b)), the "best" decentralized controller (fig. 18(c)), and the "best" nearly centralized controller (fig. 18(d)). (See ref. 14.) As expected, the centralized controller produced a faster attenuation of the structural vibration than did the decentralized controller. However,

for a given future spacecraft, the greater simplicity and fault tolerance of decentralized controllers, together with the limited on-orbit processing power, can result in selection of the decentralized controller architecture over a centralized approach. (See ref. 14.)

At ACES, the Harris researchers chose not to use the finite-element model for controller design; instead, they developed state-space models of the four dominant transfer functions by using the Eigensystem Realization Algorithm (ERA) developed at LaRC. (See ref. 15.) These models were used to independently design controllers for the four dominant control loops, which are shown in figure 19. The two IMC loops and two AGS loops each used a single sensor for feedback, as indicated by the bold arrows in the figure. Only minimal additional response information was gained by feeding back sensor signals indicated by the lighter lines in the figures. Controllers from these dominant loops were subsequently integrated into a decentralized architecture. The Harris team was one of the first to use the ACES facility, and the loops they identified were subsequently used by other researchers.

As a result of the transitional state of the LMED's during the early testing and difficulties in obtaining identified models from these devices because of their stroke limitation, the Harris team did not use ERA to develop input-output transfer functions on which to base LMED controllers. Instead, classical concepts were used, together with crude models, to design simple controllers that fed back the collocated LMED accelerometers to the corresponding LMED force axes. Each of these SISO controllers consisted of a high-pass filter cascaded with a low-pass filter.

Tests were first performed with subsets of the feedback loops previously described. In particular, the subsets applied were only the SISO IMC controllers, or only the SISO AGS controllers, or only the SISO LMED controllers. Figure 20 shows typical experimental results from ACES that illustrate the resulting performance improvement when the controllers were integrated. The additional integration of the LMED controllers resulted in only a slight improvement in performance. (See ref. 16.) The total number of states for the decentralized integrated controller was 28.

The Harris research emphasized the importance of controller simplicity—achieved through a decentralized, reduced-order controller architecture—to accommodate on-orbit processing limitations. Controller complexity can then be increased, as needed, to improve performance.

Massachusetts Institute of Technology

Using generalized parity relations, Wallace Vander Velde demonstrated sensor and actuator failure detection and isolation (FDI). This method was selected because it applies to sensors and actuators alike and does not require a hypothesis concerning possible modes of failures; thus, the computational effort required is reduced.

The generalized parity relations method produces a scalar residual $r(t)$ that is 0 only in an ideal system, where measurements are noise-free, the system is modeled accurately, and all sensors are functioning perfectly. With real (nonideal) systems, the goal is to ensure that the residual produces an identifiable signature when a sensor fails, one that is distinctive from the background noise created by unmodeled dynamics and actual measurement noise. (See ref. 17.)

Simulated sensor failures for the FDI studies were performed by adding noise to the experimental data from a given sensor or by setting the signal to 0. At Mini-MAST, sensor failures were simulated for displacement sensors, rate gyros, and accelerometers. Figure 21(a) shows the output from tip-displacement sensor 1 at vertex A, bay 18. A small amount of noise was added beginning at sample number 200. While not detectable in the sensor signal, the failure due to added noise was evident in the residual from a single-sensor parity relation (SSPR), as shown in figure 21(b).

Single-sensor parity relations have distinct limitations, however, when compared with double-sensor parity relations (DSPR's). While SSPR's are simpler to create and implement and the isolation of the faulty sensor is trivial because only one sensor is involved, the magnitude and duration of the failure signature with SSPR's can be inadequate if the sensor fails in the off mode. For example, the short-lived transient from an SSPR may be insufficient to reliably identify the failure of tip-displacement sensor 1 at sample number 200 in figure 22(a). The residuals of DSPR's for the same failure of sensor 1 to the off mode are shown in figures 22(b), 22(c), and 22(d), where the subscripts on the residuals indicate the two displacement sensor readings used in the DSPR. The failure is evident in both r_{12} and r_{13}; however, the r_{23} residual does not present such a signature because neither sensor 2 nor sensor 3 had failed (ref. 17).

Several other characteristics of parity equations were highlighted by Vander Velde's Mini-MAST research. First, although parity equations can be derived from a state-space model of the system dynamics through use of an autoregressive technique, those identified directly from experimental input-output

data performed more effectively by eliminating errors in modeling the dynamics of the structure. Increasing the sampling period and the number of time lags used in the equations also increases the magnitude of the failure signature of the residual, whether SSPR's or DSPR's are used (ref. 17). These techniques were successfully applied to accelerometer and rate gyro signals from the Mini-MAST by use of DSPR's. Distinctive failure signatures for an off failure mode are shown in figure 23(a) with two accelerometers and in figure 23(b) with an accelerometer and a rate gyro.

The research activity was not as successful in identifying failed actuators. All parity relations use both input $u(i)$ and output $y(i)$ signals, or actuator and sensor signals, whether the parity relation is looking for a sensor failure or an actuator failure. Figure 24(a) shows the single-actuator parity relation (SAPR) residual from a Mini-MAST actuator failure at sample number 250, where no distinct signature is detectable. Figure 24(b) shows the portion of that residual attributable to the $y(i)$ terms, or the nonfailed sensors, forming the background noise against which the residual from the failed actuator must be detected. Figure 24(c) shows the portion of the residual attributable to the $u(i)$ term, from the failed actuator, with a magnitude so much smaller that it is completely masked by the nonfailed sensor noise.

At the ACES facility, rate gyros and accelerometers were also used in DSPR's. Rate gyros performed well when coupled with another rate gyro, as shown in the effective DSPR signature in figure 25(a). However, even with long-time sample periods and high numbers of time lags, DSPR's using accelerometers on the ACES testbed produced only short-lived transient signatures whether coupled with another accelerometer or with a rate gyro. The short transient signature in figure 25(b) from a DSPR using a rate gyro and an accelerometer is not adequate for reliably identifying sensor failure.

Several FDI conclusions are drawn from Vander Velde's work. First, DSPR's are favored for FDI to increase the reliability of the failure detection, even though these DSPR's use decision logic to isolate the failed sensor. Also, increasing time lags and sample periods can improve the quality of the failure signature. The need for additional research has been identified with respect to failure detection of actuators.

Purdue University

Robert Skelton used modal cost analysis (MCA) with output variance constraint (OVC) controller design to develop MIMO controllers that were designed to satisfy the given inequality constraints imposed by physical limits of the hardware (such as sensor-actuator saturation levels and motion-limit sensors). An iterative procedure was applied that integrated both system modeling and control law development. Model order reduction was accomplished by using controller performance as a criterion; that is, a controller was sought to satisfy the constraint objectives with minimum control effort. In this manner, the appropriateness of the analytical model for a particular controller design was ensured. Hence, the controller was model based and the model parameters, through an iterative process, were adjusted for controller performance.

Modal cost analysis, which provided the basis for model order reduction, includes a closed-form solution for the weighted modal costs associated with the norm squared of the chosen system output vector. Controller design was integrated through the use of an output weighting matrix $\mathbf{Q}$ obtained through application of the OVC control design algorithm. Using an updated $\mathbf{Q}$ as a design parameter in the MCA creates a more appropriate reduced-order model for controller design. Design specifications and noise covariance are considered design parameters for OVC controllers. Specifications influence the weight $\mathbf{Q}$ and the model reduction and thereby influence control gains and input signals. The iterative process (fig. 26) acts as an off-line self-tuning mechanism, producing a series of controllers from low-to-high gain. The evaluation model is used for checking stability and performance, and the most appropriate controller of the series is thus selected. The corresponding $\mathbf{Q}$ becomes the weight of the output cost function for a new MCA model reduction. When the modes for the new design model are the same as those for the previous design model, $\mathbf{Q}$ is considered to have converged.

At Mini-MAST, Skelton initially used the finite-element model provided by LaRC as the evaluation model and developed design models from it via MCA. Later, he developed additional evaluation models by applying the Q-Markov covariance (QMC) equivalent realization algorithm to experimental data. QMC models based on white noise excitation differed substantially from other QMC models based on pulse excitation. This difference was due to system nonlinearities, such as joint stiction or actuator hysteresis, that were more or less averaged by the dither effect of white noise inputs. Hence, both models were appropriate for the different inputs. The pulse-based models were selected because their excitation signal more closely represented the closed-loop excitation to be used.

Table 2. Output Variance Improvements

Sensor	Response units	Open-loop variances	Closed-loop variances	Relative improvement, percent
BGYRO-X	$(\text{rad/sec})^2$	4.7998×10^{-3}	2.0794×10^{-3}	56.677
BGYRO-Y	$(\text{rad/sec})^2$	1.3490×10^{-3}	1.3540×10^{-3}	−0.602
BGYRO-Z	$(\text{rad/sec})^2$	7.1636×10^{-5}	8.0227×10^{-5}	−11.993
DET-X	m^2	5.2624×10^{-2}	1.5462×10^{-2}	70.618
DET-Y	m^2	2.1897×10^{-1}	5.0076×10^{-2}	77.132
LMED1-X	$(\text{m/sec}^2)^2$	8.3389×10^{-1}	2.9334×10^{-1}	64.822
LMED1-Y	$(\text{m/sec}^2)^2$	4.4082×10^{0}	1.2692×10^{0}	71.209
LMED2-X	$(\text{m/sec}^2)^2$	3.9487×10^{-1}	2.2573×10^{-1}	42.834
LMED2-Y	$(\text{m/sec}^2)^2$	1.6150×10^{0}	6.7444×10^{-1}	58.240

Because displacement sensors are generally not available in space, only platform-mounted accelerometers and rate gyro sensors were used for feedback on the Mini-MAST testbed. Displacement sensors, however, were used for evaluation of controller effectiveness. Test results showed that the low-frequency first bending modes had less active damping added to them than the second bending modes and the first torsion mode. Figure 27 shows open- and closed-loop responses of a displacement sensor at the mid plate as dashed and solid lines, respectively. The high-frequency second bending mode attenuated within 2 sec, but the low-frequency first bending mode did not attenuate for nearly 9 sec. Skelton attributed the less-effective active damping of the first bending mode to the particular OVC design requirements used. For instance, to satisfy the physical displacement limits (used in the OVC design), the torsional motion was much more critical than the bending motion. Using a different set of performance limits in the OVC design may also have added more control to the first bending mode. Through analytical studies, Skelton added significantly more damping to the first bending modes by using displacement sensors for feedback signals. However, for his experimental tests, Skelton chose to restrict sensors to those more likely to be available in space.

At the ACES facility, Skelton used experimentally identified modal models for developing controllers. He again chose pulse-based QMC models over those based on white noise excitation because system nonlinearities caused differences in the resulting models. All ACES sensors correlated well with potential sensors for space applications, so appropriateness of sensor selection was not an issue. With the application of Skelton's iterative procedure, a series of high-order MIMO controllers was designed. Figure 28 shows the results from a 44th-order controller. Figures 28(a) and 28(b) compare the open- and the closed-loop response of the optical detector DET-X in the IMC loop with a pulse excitation at the base excitation table, BET-X. Figure 28(c) presents simulated closed-loop responses, indicating the accuracy of the QMC models. Table 2 lists the output variance improvements for all ACES sensors due to the same controller (ref. 18).

One of the major contributions from Skelton's research is the iterative algorithm, combining system identification and control law design to produce a better model from which to design a particular controller. In addition, the self-tuning design mechanism provided through OVC produces a series of low-to-high gain MIMO controllers; thus, the mechanism improves the safety of laboratory application with expensive test articles.

Phase I Research Conclusions

Two conclusions that can be drawn from the combined research experiences of the participants in phase I of the GI program are (1) the need for accurate modeling of the entire system (not just the structure) and (2) the importance of experimental validation of control design theories. Four of the five guest investigators designing control laws directly addressed system identification and modeling. Methods for handling modeling errors and uncertainties were also addressed, but control law instabilities or other forms of unsuccessful application of control design theories still occurred in numerous instances. These occurrences highlighted the need to improve the

design model and increase the robustness of control theories. The guest investigators regarded system identification as an integral part of both the control law design process and the FDI parity equations development process. In fact, on-orbit identification was recommended as a requirement for future flight programs, which in turn requires that adequate sensors be incorporated for on-orbit measurements.

Ground testing and experimental validation of control design theories also proved essential. Theoretical guarantees of stability only relate to the analytical models (and assumed error bounds) and never promise stability of the real system. Control design techniques that appear promising on one testbed can be less successful on another. A practical demonstration of a method on a realistic testbed provides the opportunity for researchers to learn the advantages and limitations of a particular theory under varying conditions.

It was evident during phase I that in this type of program researchers tend to select their favorite control design theory and present results from effective controllers created by application of that theory. Such demonstrations, however, do not validate the theory. To enhance what can be learned from experimental applications, researchers must explore the boundaries of the theory, its limitations, and the accuracy with which the results can be predicted. Future programs can be enhanced by requiring such investigations by participants.

More comprehensive exploration of various control theories requires advanced test facilities that accommodate flexibility in pretest simulations and control law application. In phase I of the GI program, the Mini-MAST facility had stringent constraints on changes to approved test plans because of the extensive pretest simulations required to protect the truss hardware. The ACES facility, however, accommodated changes on a nearly instantaneous basis. Even though stringent testing requirements can limit the explorative approach, it is within such a highly restrictive environment that flight programs operate.

Future Phases and Plans

The GI program is designed as a multiphase research activity utilizing the Government's most advanced test facilities for experimental validation in the advancement of CSI technology. In June of 1989 with phase I well underway and with a new generation of enhanced testbeds in development, a solicitation for phase II of the CSI guest investigator program was issued. The Air Force Phillips Laboratory joined NASA for this phase and thus strengthened and extended the GI program by providing a testbed at Edwards Air Force Base. Phase II will provide three unique and challenging ground test facilities at LaRC, MSFC, and Edwards for experimental validation of the proposed CSI research.

Phase II Selection

When the NASA Research Announcement was issued, over 100 proposals were received in response to the solicitation. This response indicated not only interest in the program but also commitment to the advancement of CSI research. Table 3 shows the five phase II selections, the primary research activitites, and the facilities to be used for the experimental testing. A description of the three ground test facilities and a brief statement of the research to be conducted during phase II follows.

Phase II Ground Test Facilities

The phase II guest investigators will use three new ground test facilities specifically designed and developed for implementing, validating, and evaluating CSI methodologies. Experiments in vibration suppression, pointing, tracking, slewing, articulation, distributed control, and system identification will be validated in these newly developed testbeds, which are described in the following sections.

Facility at Langley Research Center. At LaRC, the CSI Evolutionary Model (CEM) is a generic ground test facility that will evolve over time in configuration, model complexity, and experimental capabilities. The testbed is designed for validation of CSI design methodology and hardware implementation with provisions for hardware changes. The initial configuration is a long truss bus with several appendages of varying degrees of flexibility. The bus consists of a 4-longeron truss, 17 m in length, that is divided into 62 cubic bays with an 11-bay laser tower and a 4-bay reflector tower. An eight-rib reflector, 5 m in diameter, is mounted on the reflector tower. A laser source, mounted atop the laser tower, allows experiments with line-of-sight (LOS) pointing accuracy. The laser beam reflects from a mirror mounted in the center of the reflector to the detector located on the laboratory ceiling. The model is suspended by 2 cables attached to 4 horizontal support trusses of 10 bays each, as shown in figure 29. (See ref. 19.)

The node-ball joints and aluminum truss tubes with special end fittings provide for ease of tube replacement as required for subsequent configurations. The CEM configuration to be used by the guest investigators was designed and developed through a cooperative integrated design effort between the controls

Table 3. Phase II Guest Investigators

University or industry	Principal investigator	Research facility	Research activity
Boeing Aerospace Company	Dean Jacot	Air Force ASTREX	CMG-RCS pointing and slewing maneuvers
Harris Corporation	David Hyland	MSFC CASES	Optimal projection for uncertain systems controller design
Martin Marietta Corporation	Eric Schmitz	LaRC CEM	Controller design with active and passive vibration suppression techniques
Massachusetts Institute of Technology	Andreas von Flotow	Air Force ASTREX	Controller design with passive damping for vibration suppression
Texas A & M University	Srinivas Vadali	Air Force ASTREX	Feedback-feedforward controller design

and structural dynamics CSI researchers at LaRC. The design addresses global LOS pointing as the primary performance measure. Future configurations will include multiple pointing instruments and will focus on the development of multiple-payload isolation technology.

The primary control actuators of the CEM are 16 single-axis, bidirectional, compressed air thrusters installed in groups of four, acting in pairs to achieve pure translational forces. Reaction wheels, piezoceramic, and visco-elastic actuation devices are planned for implementation during the testbed evolution. More than 200 sensors are used on the testbed: 18 servo accelerometers and 9 angular rate sensors serve as control feedback sensors, 195 lightweight accelerometers provide system identification measurements. The real-time computer system is an enhanced Digital Equipment Corp. VAX 3200 interfaced to a CAMAC data acquisition system. A typical controller (40 states, 8 inputs, and 8 outputs) executes at a rate of 250 Hz. The real-time computer is connected to the CEM hardware via a fiber-optic link (ref. 19).

Facility at Marshall Space Flight Center. The Controls, Astrophysics, and Structures Experiment in Space (CASES) ground test facility at MSFC uses the 32-m Solar Array Flight Experiment (SAFE) boom hardware, which was flown on the STS-41D Shuttle mission. A 2- by 2-m plate, held in place by bungee cords, is mounted at the boom tip. The inverted boom (fig. 30) is secured to a support structure, which in turn is attached to an airbearing tripod system that translates in the horizontal plane and rotates about the longitudinal axis (ref. 9). This facility can support investigations of many CSI aspects of large space structures such as vibration suppression, deployment and retraction, and sensor and actuator performance. The boom is equipped with 11 sensors and 7 actuators. Control authority of the test article is provided by bi-linear thrusters (BLT's) at the boom tip, two single-axis angular momentum exchange devices (AMED's) at a midpoint on the boom, three single-axis AMED's at the boom tip, and a tip roll motor. The performance measurement feedback is provided by angular velocity sensors at the base, midboom, and tip; acceleration sensors at the base and tip; boom angular velocity sensors; a tip-displacement sensor for position and angle measurement of the tip plate; and an optical sensor system (ref. 9).

Two Unholtz-Dickie shakers form a disturbance system with three degrees of freedom: two translational degrees of freedom and a torsional degree of freedom. An interface system between the test article and the disturbance system, the Mission Peculiar Experiment Support Structure (MPESS), simulates a Shuttle and payload interface. The real-time computer system, a SUN Microsystem workstation host and a Sky Computers, Inc., Warrior array processor, can accommodate a 100th-order controller with 64 inputs and 64 outputs at a sampling rate of 250 Hz (ref. 9).

Facility at Air Force Phillips Laboratory. The Air Force Advanced Space Structures Technology Research Experiments (ASTREX) ground test facility is located at the Phillips Laboratory, Edwards

Air Force Base, California. ASTREX is a three-axis large angle retargeting facility designed for the demonstration and evaluation of large angle slewing and subsequent pointing and shape control of a variety of flexible bodies. The ASTREX experiment article (fig. 31) is a graphite/epoxy, dynamically scaled model of a three-mirror, space-based laser beam expander designed by Boeing Aerospace Company. The structure is supported by a spherical air bearing, mounted atop a pedestal that provides the test article with three degrees of angular freedom. The modular design allows the initial tubes to be replaced with passive damping treatments and embedded sensors and actuators. The test article consists of a primary segmented mirror, a secondary mirror supported by three ACESA struts developed by TRW, Inc., and a tertiary mirror. (See the schematic in fig. 32.) Mass simulators for the tertiary mirror and two tracker telescopes are attached to the primary support truss (ref. 20).

The test article is housed in a constant-temperature air-tight enclosure to minimize disturbances. An extensive complement of sensors and actuators, which can be relocated, is available for system identification, rapid retargeting, pointing and shape control, and active vibration suppression. The instrument complement used can be selected from among throttle-controlled cold-gas thrusters, proof-mass actuators, reaction wheels, control moment gyros, accelerometers, optical line-of-sight sensors, and embedded sensors and actuators. A real-time control and data acquisition computer system, developed for ASTREX by Integrated Systems, Inc., can support user-defined sampling rates up to 1500 Hz. A typical controller is of 40th order with 32 inputs and 32 outputs at a sampling rate of 250 Hz. Multiple processors provide sustained calculations of 10 to 15 MFLOPS (million floating-point operations per second). (See ref. 20.)

PHASE II Research Objectives

The phase II guest investigators from the five selected institutions will use the three CSI ground test facilities described in the previous section. Unlike phase I of the GI program, these five research teams will only use a single facility for the duration of their research activities, which are described in the following sections.

Boeing Aerospace Company. The Boeing Aerospace & Electronics Company proposed research to demonstrate precision pointing and slewing of an optical satellite structure under control moment gyroscope (CMG) and reaction control system (RCS) control. The ASTREX ground test facility will be used for validation testing and demonstration. This proposal offers a unique combination of Boeing-owned, high-precision, and high-control authority CMG's and the ASTREX facility designed as a realistic test article with a large-angle motion capability for slewing and precision pointing. The comprehensive experimental plan includes new investigations blending precision pointing and CMG-RCS slewing, which builds on past Boeing experience. The proposed program will advance the understanding of CMG-shaped torque slewing, anti-singularity CMG control laws, CMG-induced vibrations, and combined CMG-RCS slewing. This research will demonstrate the feasibility of precision pointing via CMG's through validation testing.

Massachusetts Institute of Technology (MIT). The MIT objective is to quantify the need, cost, and benefit of passive damping treatments in terms of their impact on CSI issues in the design and performance of spacecraft. The validation activity will be conducted on the ASTREX ground test facility. Optimally damped components will be developed and tested on the ASTREX hardware by interchanging existing truss members and the damped members. The design goal is to increase the damping ratio while not changing other testbed dynamics. The proposed research will permit a relatively straightforward comparison between active control performance of optimally damped structures and thereby advance the understanding and feasibility of interchanging optimally damped components with existing hardware members on flight test articles. The damping mechanisms to be investigated and the manner of implementing the damping materials into the structure will greatly extend the knowledge of the CSI community in the effective design of optimally damped truss components.

Texas A&M University. Texas A & M proposes to develop and implement control laws on the ASTREX ground test facility. The major activity involves comparing two distinctly different types of actuators, cold-gas thrusters, and single-gimbal control moment gyroscopes, for the implementation of real-time control laws. Torque-shaped feedback controllers will be developed and used in conjunction with each other to provide near-minimum-time maneuver capability and robust global stability. This practical approach will advance the knowledge of implementing real-time controllers using different actuators in parallel to provide greater maneuverability and stability.

Harris Corporation. The research objective of the Harris Corporation is to examine both

analytically and experimentally the major trade-offs in the design of active feedback controllers, including performance versus processor throughput (sample rate and controller complexity), performance versus robustness (tolerance to modeling uncertainty), and performance versus degree of decentralization. The Harris control theory approach, OPUS, was specifically developed to address the constraints of space-qualified hardware as well as uncertain structural modeling. The experimental testing will be conducted on the MSFC CASES ground test facility. The results of this research will provide a reliable integrated methodology examination of the major design trade-offs in active control-system synthesis.

Martin Marietta Corporation. The Martin Marietta research focuses on two areas: (1) the integration of system identification techniques with robust control design methods to provide high-performance closed-loop pointing control systems and (2) the integration of active and passive damping vibration suppression techniques to produce control systems that are simpler, more reliable, and less sensitive to modeling uncertainties than current damping systems. Validation tests will be conducted on the LaRC CEM test facility. Several control design methods will be evaluated analytically and validated against the modal data obtained from the CEM. The synergistic benefits of the combined passive and active vibration suppression techniques will also be evaluated on the CEM with a modular, removable, passive damping system developed by Martin Marietta. The proposed research will provide the CSI community with a clearer understanding of the significant advantages offered by the most promising control theories, validated by real-time test results obtained on an advanced CSI testbed. The application of integrated active and passive damping to the CEM will add a new dimension toward reliable, predictable damping design and implementation, and this dimension is critical to the success of future space missions.

Concluding Remarks

The objective of the NASA Controls-Structures Interaction (CSI) Program is to integrate the design of the control system and the structure of large, flexible spacecraft to meet the system performance requirements of future space missions. The three field centers cooperatively developing CSI technology are the Langley Research Center (LaRC), the Marshall Space Flight Center (MSFC), and the Jet Propulsion Laboratory (JPL). The Air Force Phillips Laboratory has become a participating member in the CSI guest investigator (GI) program.

Phase I of the GI program has recently completed a 2-year activity. Six guest investigator teams, using ground test facilities at LaRC and MSFC, conducted experiments to validate CSI techniques in system identification and controls development. The objective of the GI program is to support CSI technology advancement by (1) soliciting and supporting CSI research, (2) providing advanced ground test facilities for experimental validation of this research, and (3) disseminating the experimental results to the research community in a timely manner.

The primary goal of all the researchers involved in the GI program was to advance CSI technology and to increase the understanding of practical limitations of simplifying theoretical assumptions. The sharing of information and experiences toward the common goal was prevalent during the 2 years. The objective of demonstrating high-performance active vibration control on realistic space structures was realized, and several methods demonstrated at least an order of magnitude increase in damping.

Three general conclusions drawn from the results of phase I of the GI program are as follows: (1) accurate modeling of the entire system, not just the structure, is necessary for a successful validation process, (2) the importance of experimental validation of control design theories cannot be over emphasized in establishing benefits and limitations of the research, and (3) full-order, multivariable controllers are not necessarily required for CSI; instead, the performance requirements and system dynamics should determine the complexity of the controller. The researchers regarded system identification as an integral part of both the control law design process and the failure detection and isolation parity equations development process. In fact, on-orbit identification was recommended as a requirement for future flight programs, which in turn requires adequate sensors be incorporated for on-orbit measurements.

The GI program has been instrumental in advancing CSI technology and in producing valuable experience to be shared with the research community. With this experience and the improved government test facilities ready for use, the phase II research effort and subsequent phases promise to result in even more impressive demonstrations. The advancements made in CSI technology and the newly developed testbeds are major steps toward enabling ground validation of integrated controls-structures design for future space structures.

NASA Langley Research Center
Hampton, VA 23681-0001
October 26, 1992

Appendix

Guest Investigators

The names, addresses, and telephone numbers of the phase I guest investigators as of November 1992 are as follows.

Arizona State University
Attn: Dr. Bong Wie
Aerospace Engineering
Tempe, AZ 85287-6106
(602) 965-8674

Boeing Aerospace Company
Attn: Dr. J. Michael Chapman
Mail Stop 82-97
P.O. Box 3999
Seattle, WA 98124
(206) 773-9554

California Institute of Technology
Attn: Dr. John C. Doyle
Electrical Engineering 11681
Pasadena, CA 91125
(818) 356-4808

Dynamic Engineering, Incorporated
Attn: Mr. W. H. Reed III
703 Middle Ground Blvd.
Newport News, VA 23606
(804) 873-1344

Harris Aerospace Systems Division
Attn: Dr. David C. Hyland
Mail Stop 22/4847
P. O. Box 94000
Melbourne, FL 32902
(407) 729-2138

Massachusetts Institute of Technology
Attn: Dr. Wallace E. Vander Velde
Room 33-109
77 Massachusetts Avenue
Cambridge, MA 02139
(617) 253-7541

Purdue University
Attn: Dr. Robert E. Skelton
School of Aeronautics and Astronautics
Grissom Hall
W. Lafayette, IN 47907
(317) 494-5132

University of Cincinnati
Attn: Dr. Randall J. Allemang
Dept. of Mechanical Engineering
Mail Location #72
Cincinnati, OH 45221
(513) 556-2725

University of Cincinnati
Attn: Dr. Gary Slater
Dept. of Aerospace Engineering
Mail Location #70
Cincinnati, OH 45221
(513) 556-3223

University of Minnesota
Attn: Dr. Gary J. Balas
Aerospace Engineering & Mechanics
107 Akerman Hall
110 Union Street SE
Minneapolis, MN 55455
(612) 625-6857

The names, addresses, and telephone numbers of the phase II guest investigators as of November 1992 are as follows.

Boeing Defense and Space Group
Attn: Dean Jacot
Mail Stop 82-24
P. O. Box 3999
Seattle, WA 98124-2499
(206) 773-8629

Harris Corporation
Attn: Dr. David C. Hyland
Mail Stop 22/4847
P. O. Box 94000
Melbourne, FL 32902
(407) 729-2138

Martin Marietta Corporation
Attn: Dr. Eric Schmitz
Mail Stop 4372
P. O. Box 179
Denver, CO 80201
(303) 971-2732

Massachusetts Institute of Technology
Attn: Dr. Andreas H. von Flotow
Dept. of Aeronautics and Astronautics
Room 37-335
77 Massachusetts Avenue
Cambridge, MA 02139
(617) 253-4865

Texas A & M University
Attn: Dr. Srinivas R. Vadali
Dept. of Aerospace Engineering
College Station, TX 77843-3124
(409) 845-3918

References

1. Report of the Panel on Future Directions in Control Theory (Wendell H. Fleming, chair): *Future Directions in Control Theory—A Mathematical Perspective.* Soc. for Industrial and Applied Mathematics, 1988.

2. Newsom, Jerry R.; Layman, W. E.; Waites, H. B.; and Hayduk, R. J.: The NASA Controls-Structures Interaction Technology Program. IAF-90-290, Oct. 1990.

3. Chapman, J. M.: *Nonlinear Modeling of Joint Dominated Structures.* NASA CR-4324, 1990.

4. Gold, Ronald R.; Friedman, Inger P.; Reed, Wilmer H., III; and Hallauer, W. L.: *Suspension Systems for Ground Testing Large Space Structures.* NASA CR-4325, 1990.

5. Adams, Louis R.: *Design, Development and Fabrication of a Deployable/Retractable Truss Beam Model for Large Space Structures Application.* NASA CR-178287, 1987.

6. Tanner, Sharon E.; Pappa, Richard S.; Sulla, Jeffrey L.; Elliott, Kenny B.; Miserentino, Robert; Bailey, James P.; Cooper, Paul A.; Williams, Boyd L., Jr.; and Bruner, Anne M.: *Mini-MAST CSI Testbed User's Guide.* NASA TM-102630, 1992.

7. Sharkey, John P.; Waites, Henry; and Doane, George B., III: *Distributed Control Using Linear Momentum Exchange Devices.* NASA TM-100308, 1987.

8. Waites, Henry B.; Irwin, R. Dennis; Jones, Victoria; Rice, Sally Curtis; Seltzer, Sherman M.; and Tollison, Danny K.: *Active Control Technique Evaluation for Spacecraft (ACES).* AFWAL-TR-88-3038, U.S. Air Force, June 1988. (Available from DTIC as AD A202 475.)

9. Jones, Victoria L.; Bukley, Angelia P.; and Patterson, Alan F.: NASA/MSFC Large Space Structures Ground Test Facility. *A Collection of Technical Papers, Volume 2—AIAA Guidance, Navigation and Control Conference,* Aug. 1991, pp. 792–806. (Available as AIAA-91-2694.)

10. Wie, Bong; Horta, Lucas; and Sulla, Jeff: Active Structural Control Design and Experiment for the Mini-Mast. *Proceedings of the 1990 American Control Conference,* Volume 2, IEEE Catalog No. 90CH2896-9, American Automatic Control Council, 1990, pp. 1428–1434.

11. Wie, Bong: Experimental Demonstration of a Classical Approach for Flexible Structure Control: The ACES Testbed. *A Collection of Technical Papers—AIAA Guidance, Navigation and Control Conference,* Aug. 1991, pp. 818-826. (Available as AIAA-91-2696.)

12. Allemang, R. J.; Shelley, S. J.; Brown, D. L.; and Zhang, Q.: Practical Experience With Identification of Large Flexible Structures. *Proceedings of the 1990 American Control Conference,* Volume 2, IEEE Catalog No. 90CH2896-9, American Automatic Control Council, 1990, pp. 1441–1444.

13. Slater, G. L.; Bosse, A.; and Zhang, Q.: Practical Experience With Multivariable Positivity Controllers. *Proceedings of the 1990 American Control Conference,* Volume 2, IEEE Catalog No. 90CH2896-9, American Automatic Control Council, 1990, pp. 1445–1448.

14. Collins, Emmanuel G., Jr.; King, James A.; Phillips, Douglas J.; and Hyland, David C.: *High Performance, Accelerometer-Based Control of the Mini-MAST Structure at Langley Research Center.* NASA CR-4377, 1991.

15. Juang, Jer-Nan; and Pappa, Richard S.: Effects of Noise on Modal Parameters Identified by the Eigensystem Realization Algorithm. *J. Guid., Control, & Dyn.*, vol. 9, no. 3, May–June 1986, pp. 294–303.

16. Collins, Emmanuel G., Jr.; Phillips, Douglas J.; and Hyland, David C.: *Design and Implementation of Robust Decentralized Control Laws for the ACES Structure at Marshall Space Flight Center.* NASA CR-4310, 1990.

17. Vander Velde, Wallace E.; and Van Schalkwyk, Christiaan M.: Failure Detection and Isolation Experiments With the Langley Mini-Mast. *Proceedings of the 1990 American Control Conference,* Volume 2, IEEE Catalog No. 90-CH2896-9, American Automatic Control Council, 1990, pp. 1422–1427.

18. Hsieh, C.; Kim, J. H.; and Skelton, R. E.: Closed Loop Lab Tests of NASA's Mini-Mast. *Proceedings of the 1990 American Control Conference,* Volume 1, IEEE Catalog No. 90CH2896-9, American Automatic Control Council, 1990, pp. 1435–1440.

19. Belvin, W. Keith; Elliott, Kenny B.; Horta, Lucas G.; Bailey, Jim; Bruner, Anne; Sulla, Jeff; Won, John; and Ugoletti, Roberto: *Langley's CSI Evolutionary Model: Phase 0.* NASA TM-104165, 1991.

20. Norris, G. A.: Initial Operational Capability of the ASTREX Large Space Structures Test Bed. *NASA/DOD Controls-Structures Interaction Technology 1989,* Jerry R. Newsom, compiler, NASA CP-3041, 1989, pp. 507–522.

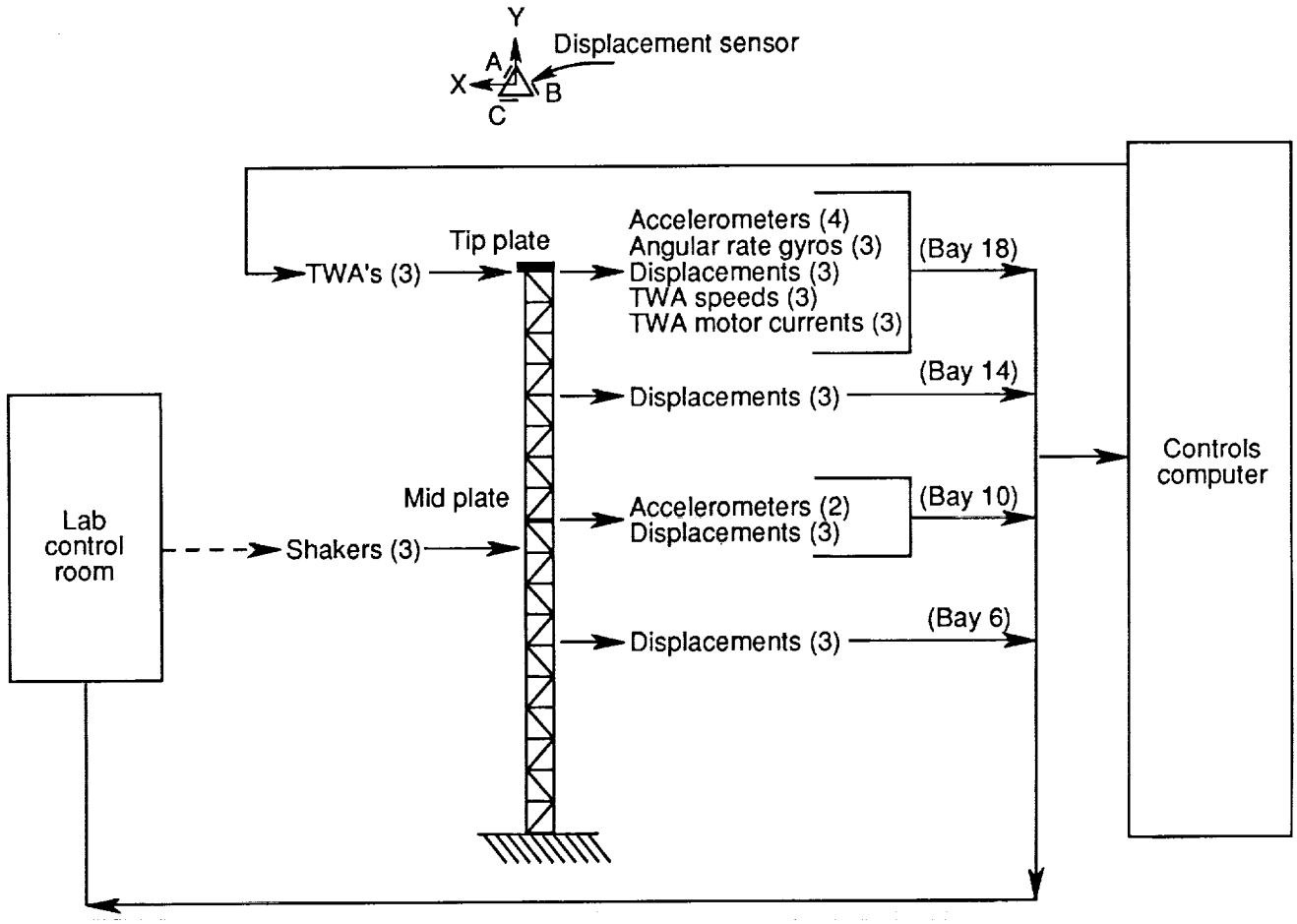

Figure 1. Mini-MAST test facility. TWA indicates torque-wheel actuator.

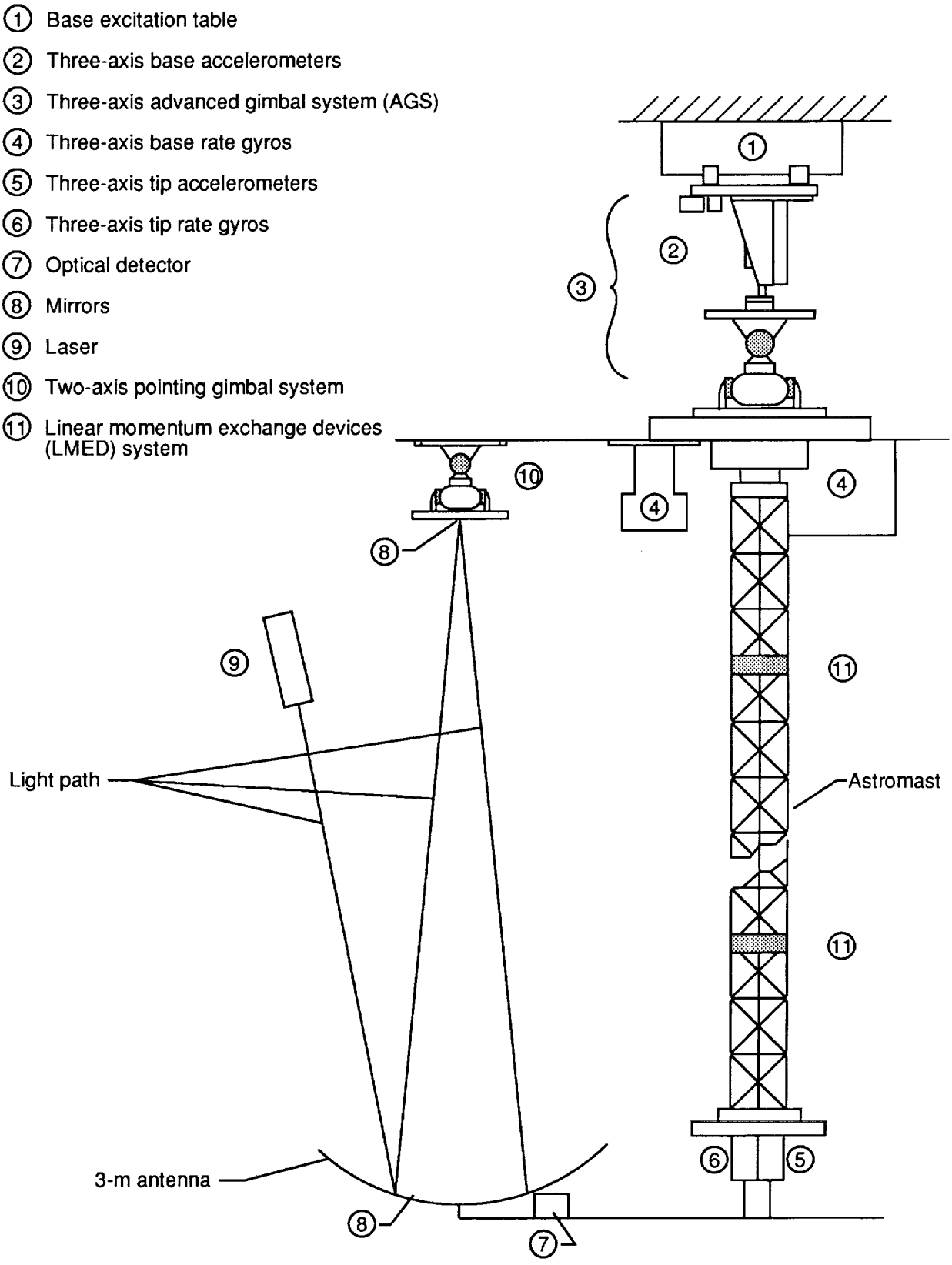

Figure 2. ACES ground test facility.

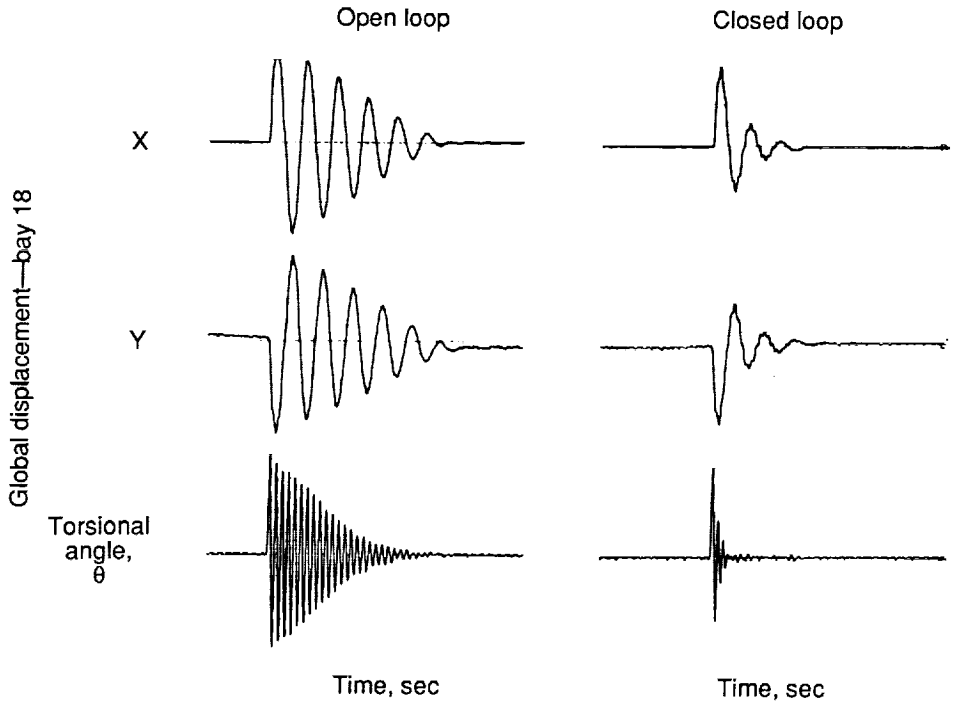

Figure 3. Open-loop and closed-loop responses of Mini-MAST collocated controller at bay 18.

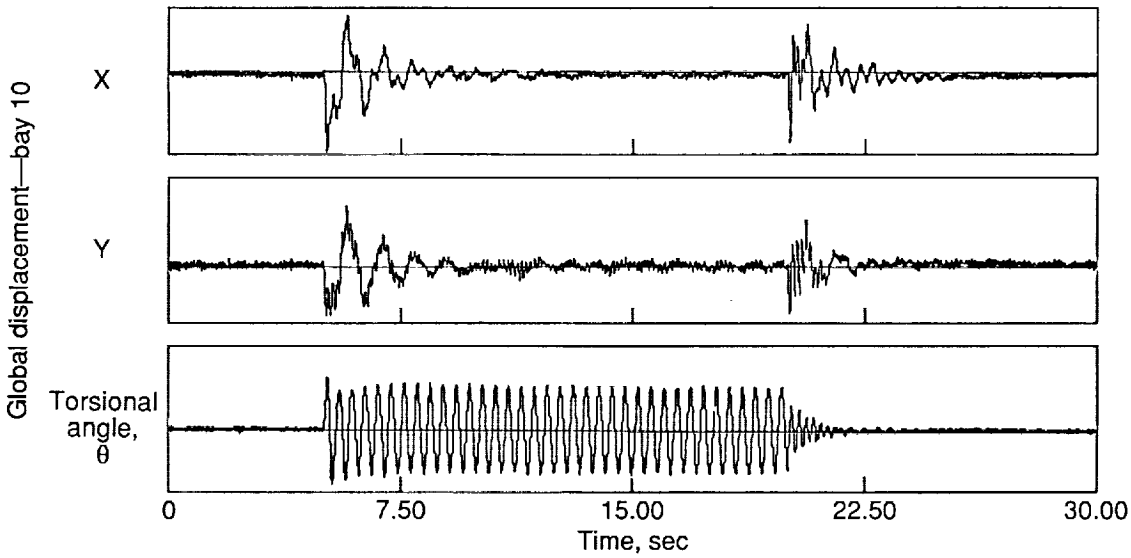

Figure 4. Closed-loop response of Mini-MAST noncollocated controller with disturbance rejection at bay 10.

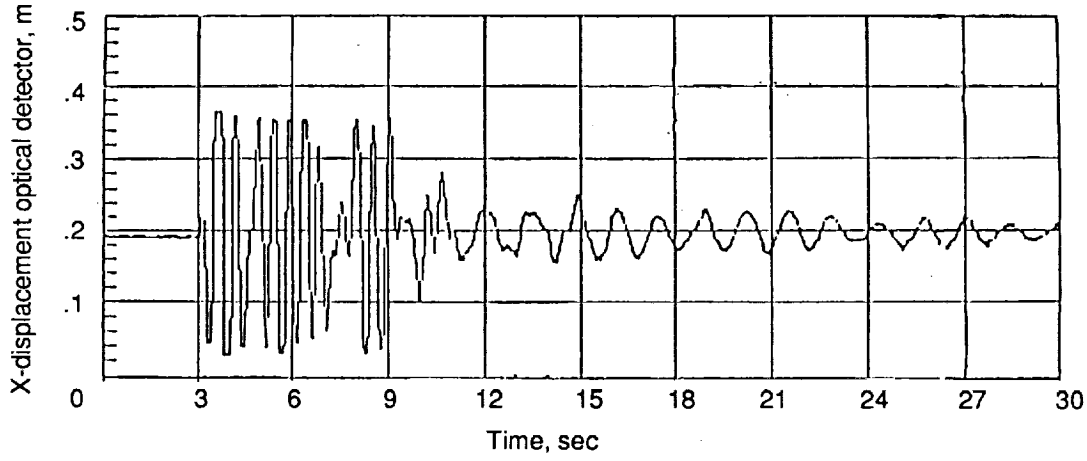

(a) Open-loop response.

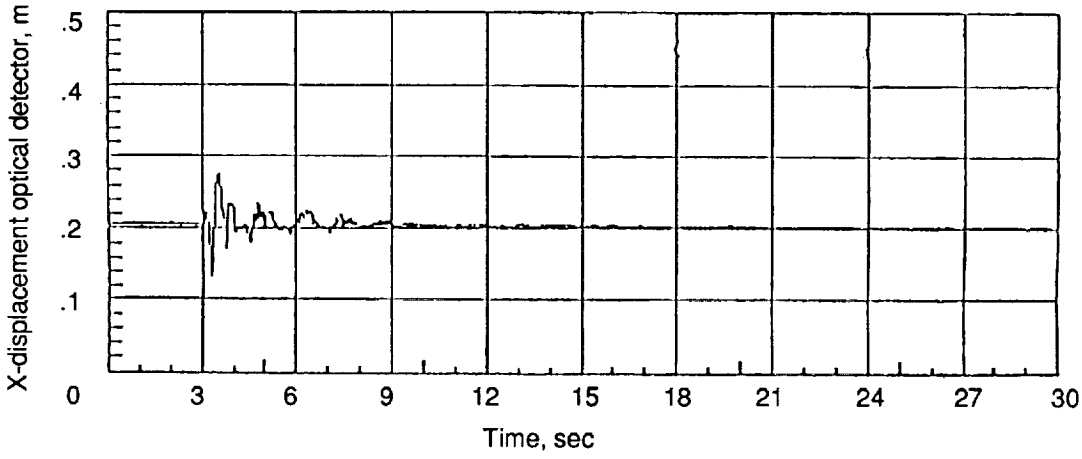

(b) Closed-loop response with integrated AGS and IMC controllers.

Figure 5. ACES experimental data for DET-X responses to BET-X pulse.

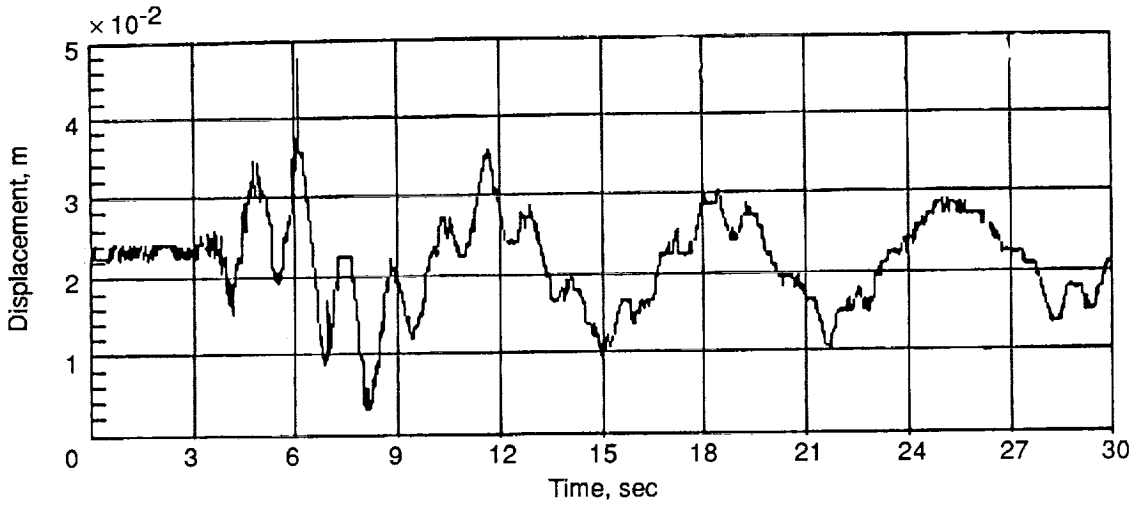

(a) Open-loop response.

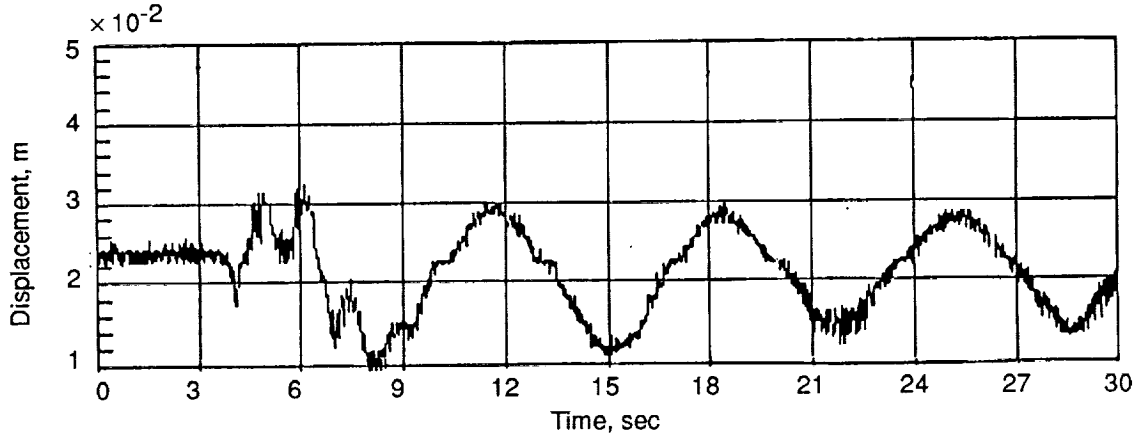

(b) Closed-loop response with integrated AGS and IMC controllers.

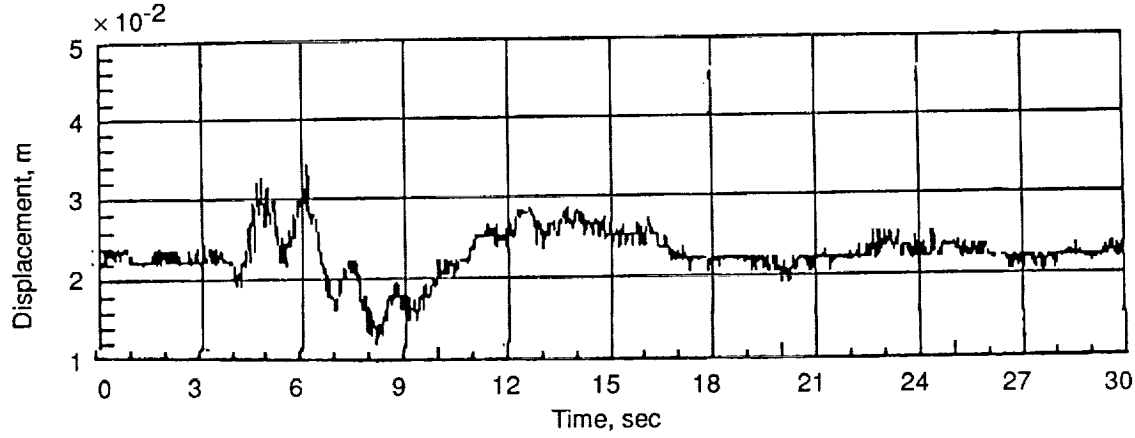

(c) Closed-loop response with dipole and integrated controllers.

Figure 6. ACES experimental data for DET-X responses to BET-X step function disturbance.

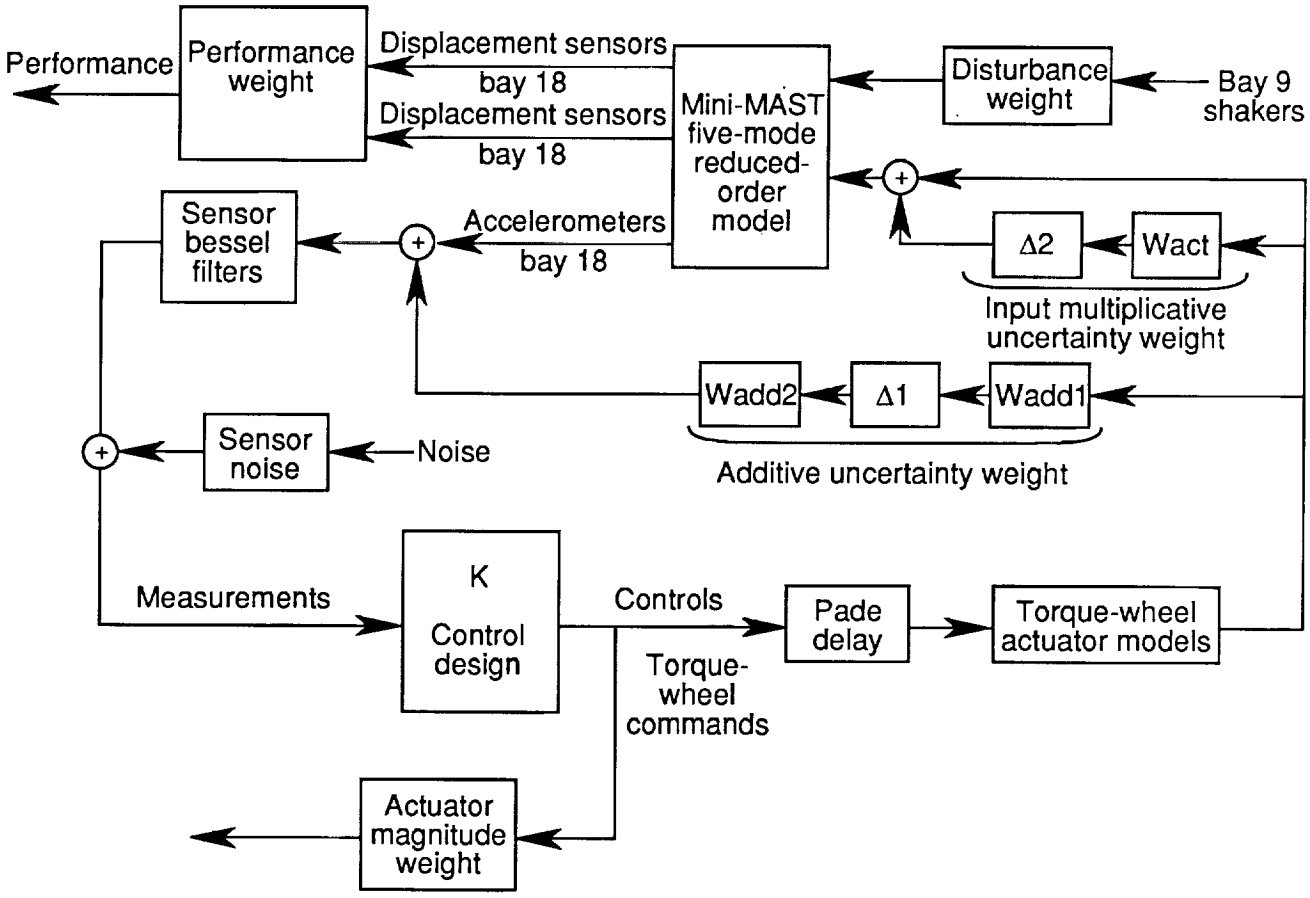

Figure 7. Mini-MAST system design diagram with uncertainties.

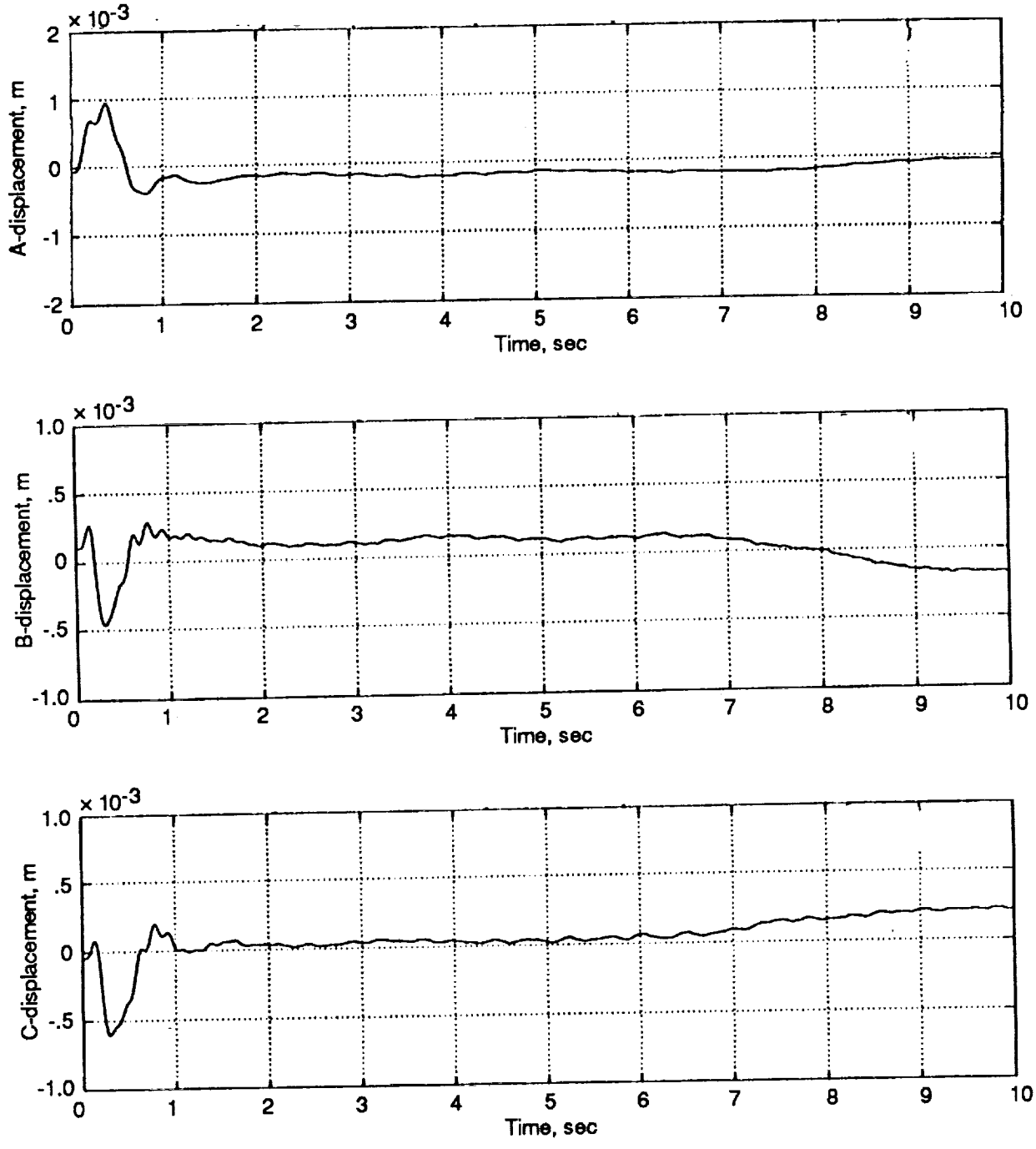

(a) Displacements A, B, and C at bay 18.

Figure 8. Mini-MAST closed-loop results for most aggressive controller.

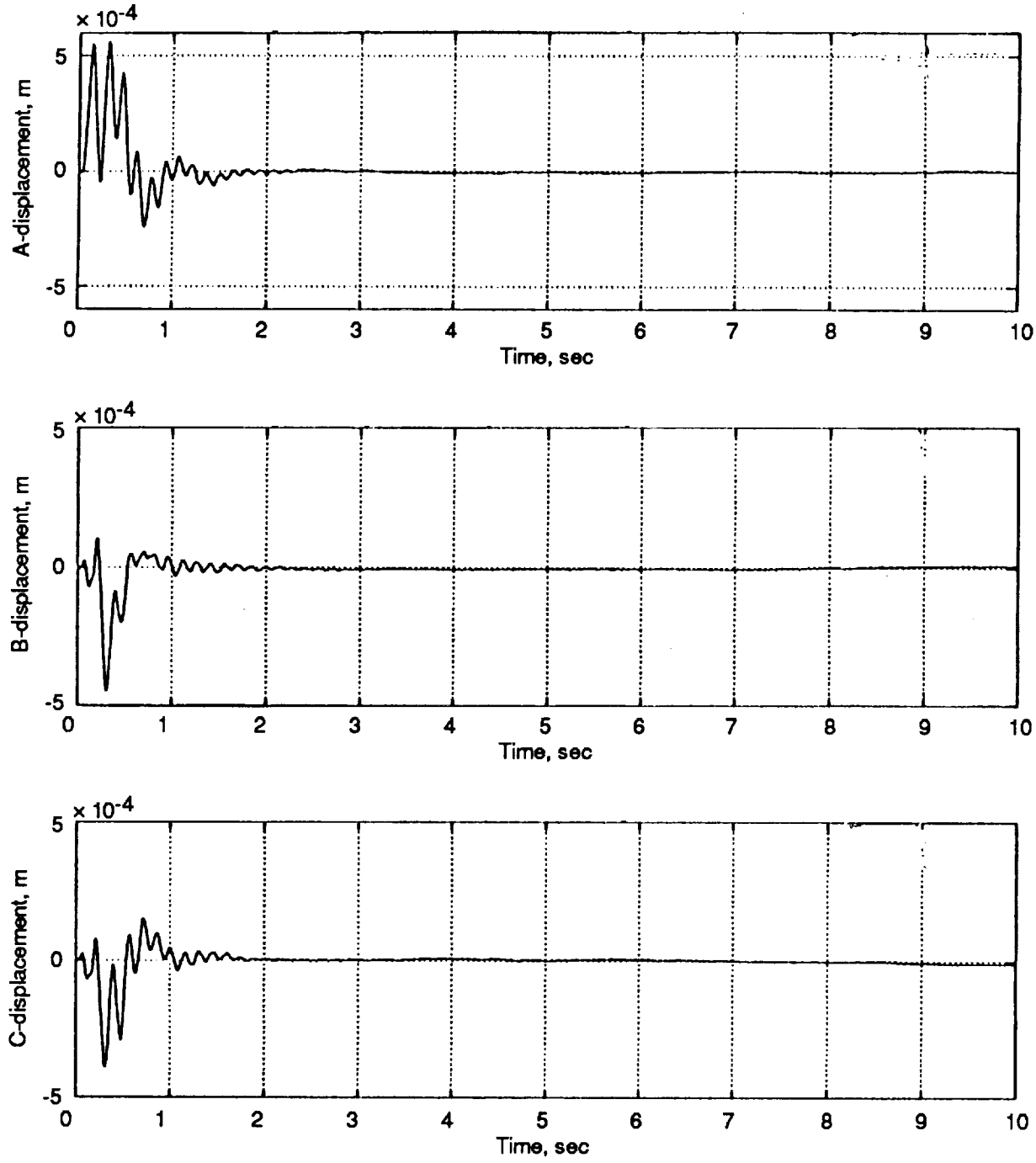

(b) Displacements A, B, and C at bay 10.

Figure 8. Concluded.

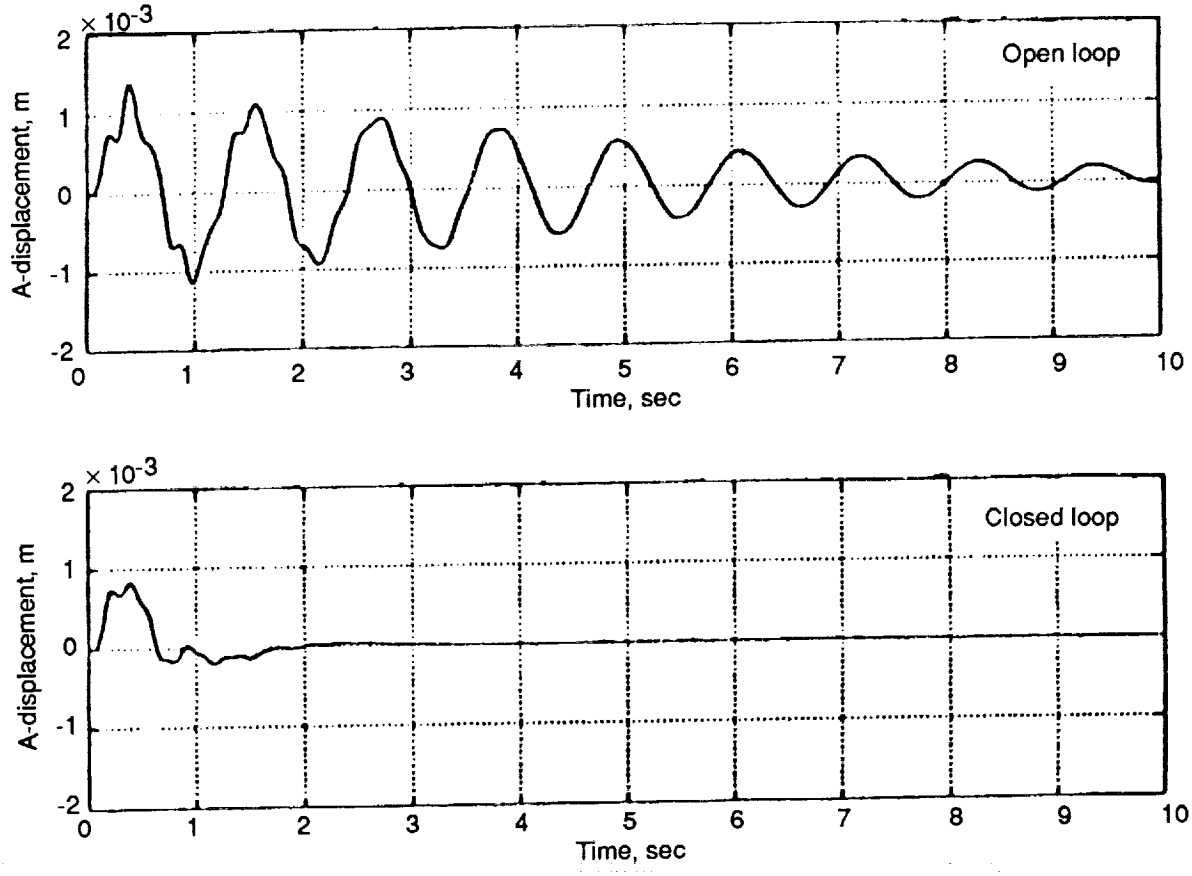

Figure 9. Mini-MAST bay 18 open- and closed-loop results from controller designed with 20-percent uncertainty.

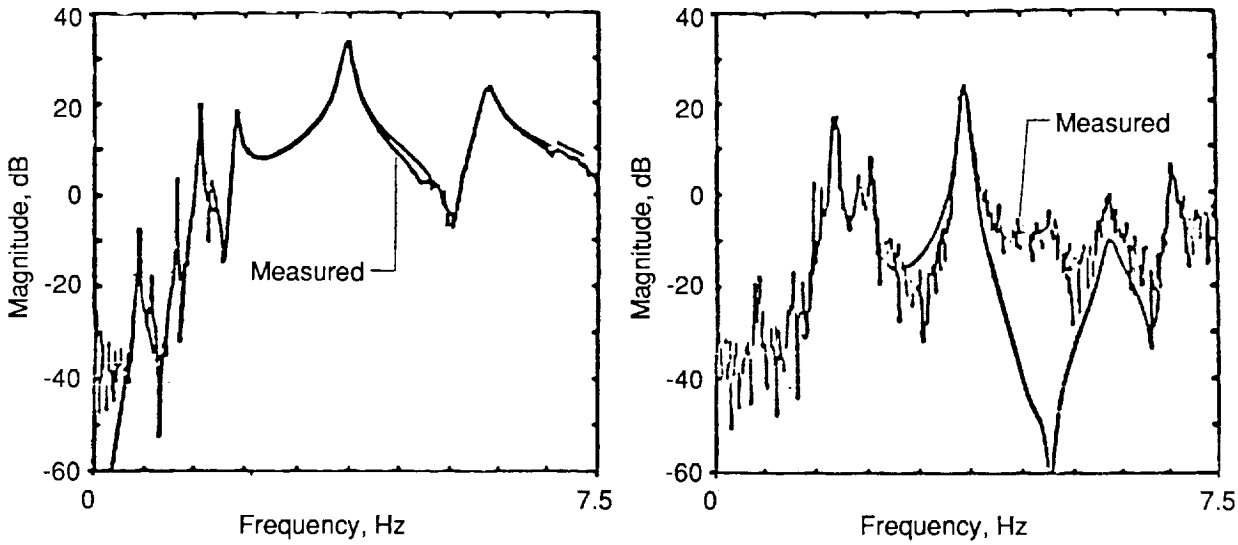

Figure 10. Measured and synthesized frequency response functions from ACES.

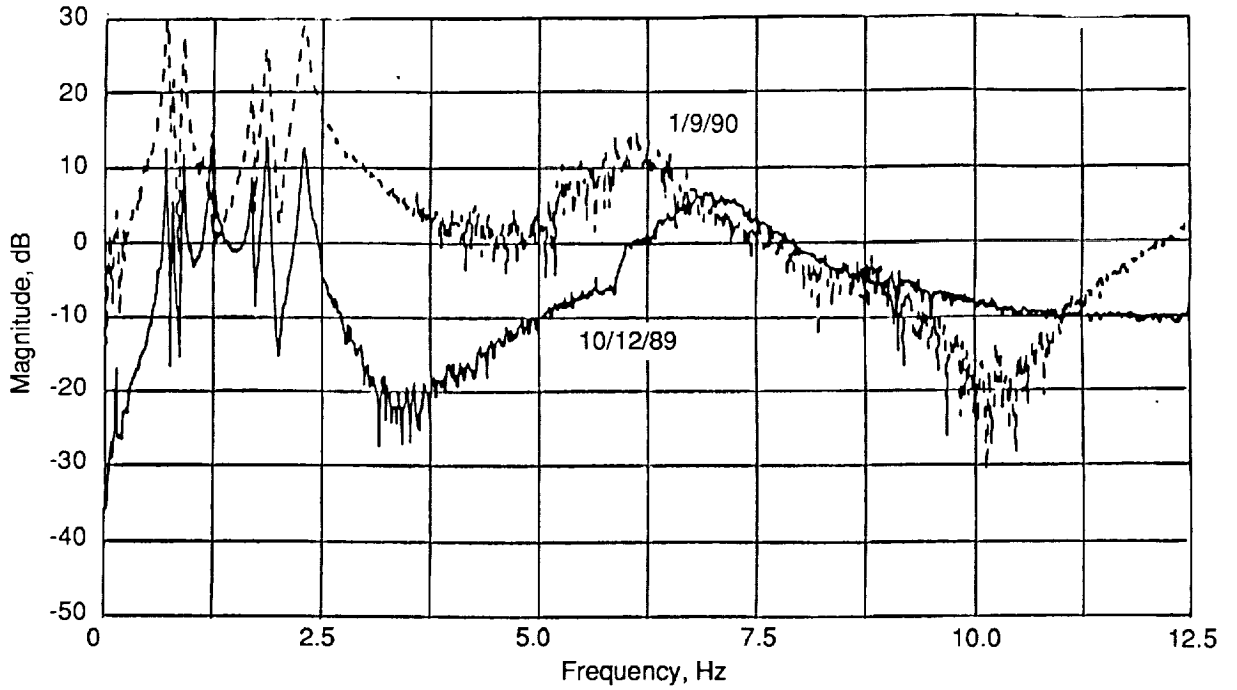

Figure 11. ACES time-variant characteristics.

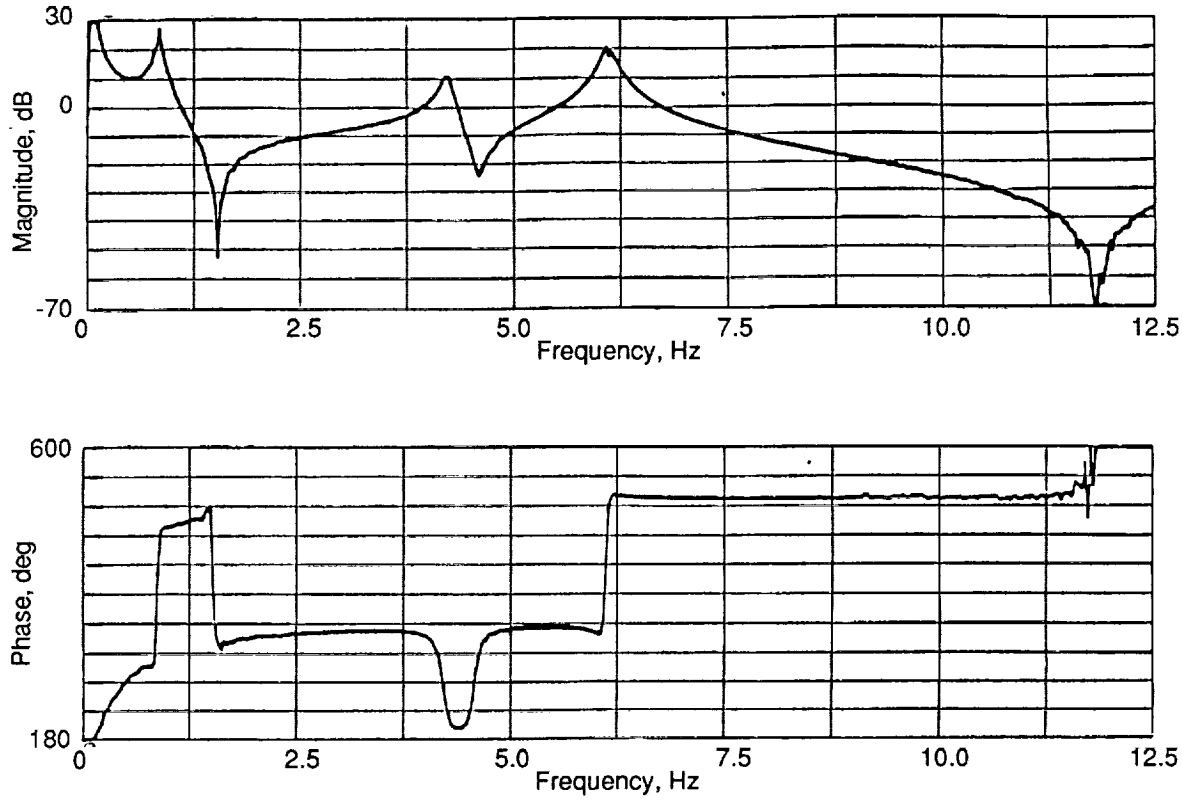

Figure 12. Mini-MAST apparent phase gain at resonance.

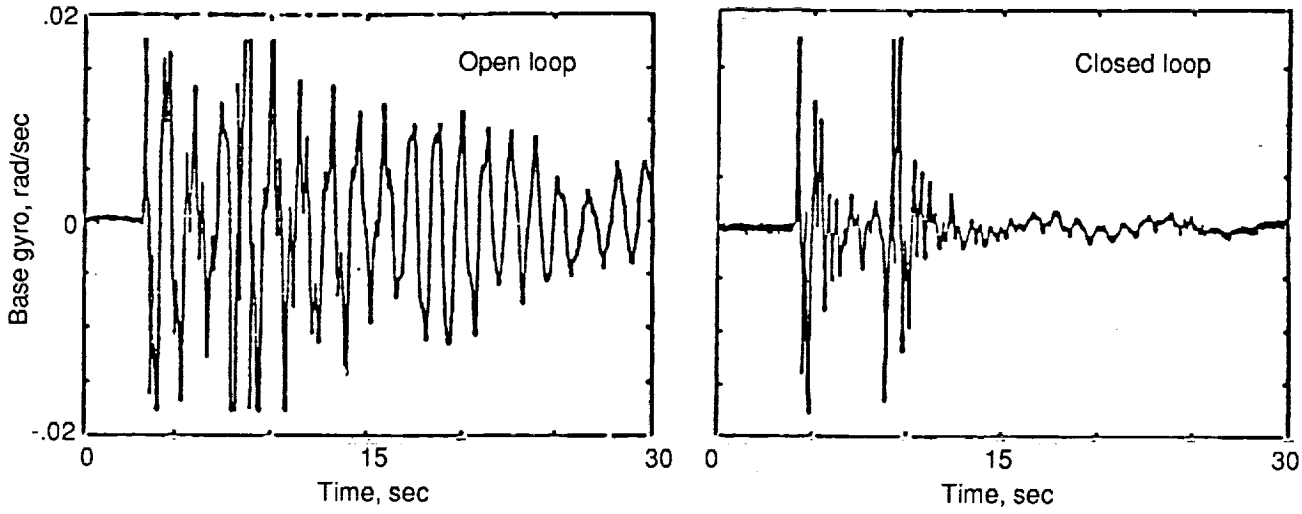

Figure 13. ACES AGS results for open-loop and closed-loop responses.

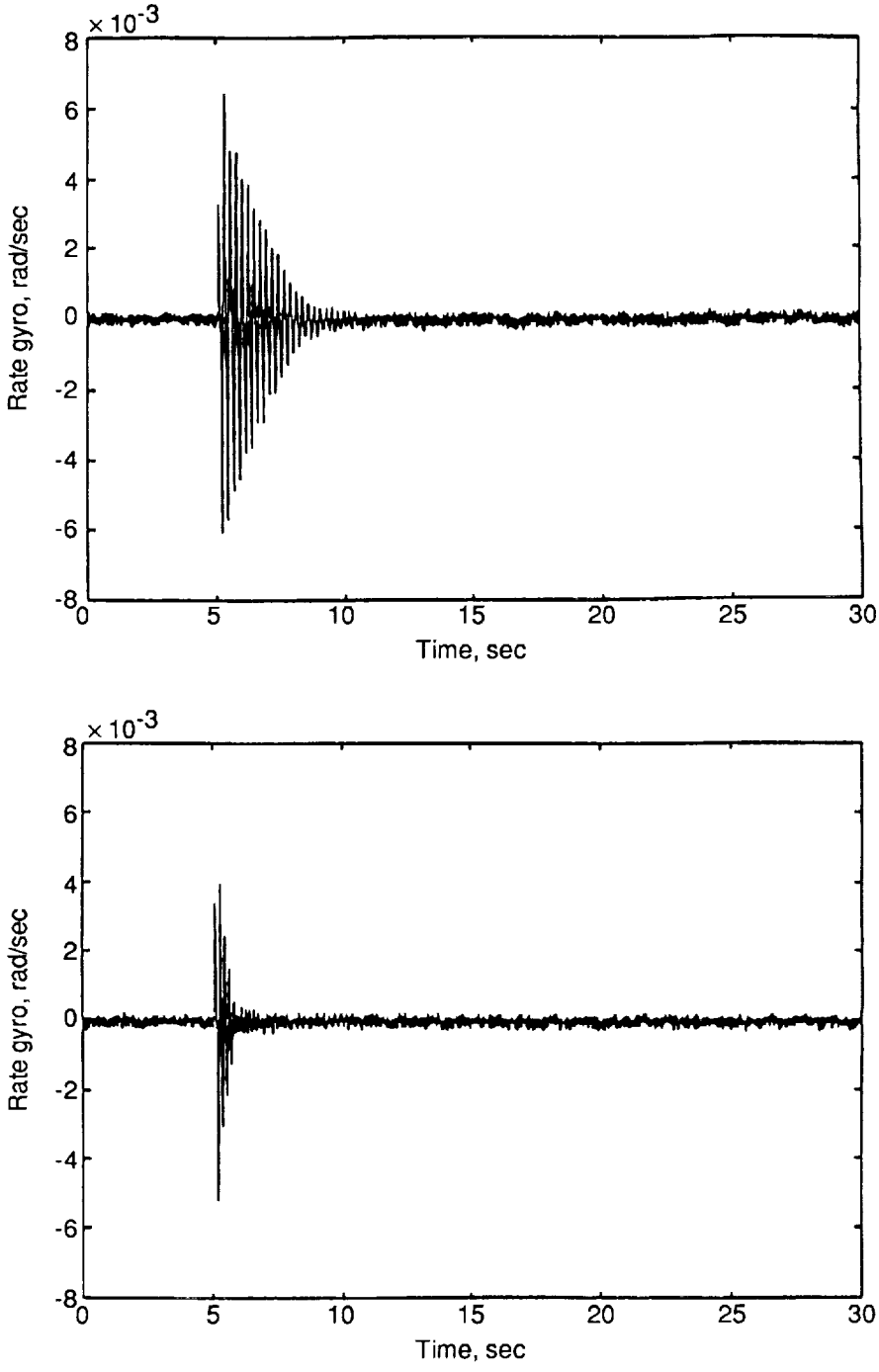

Figure 14. Mini-MAST open- and closed-loop responses for SISO controller.

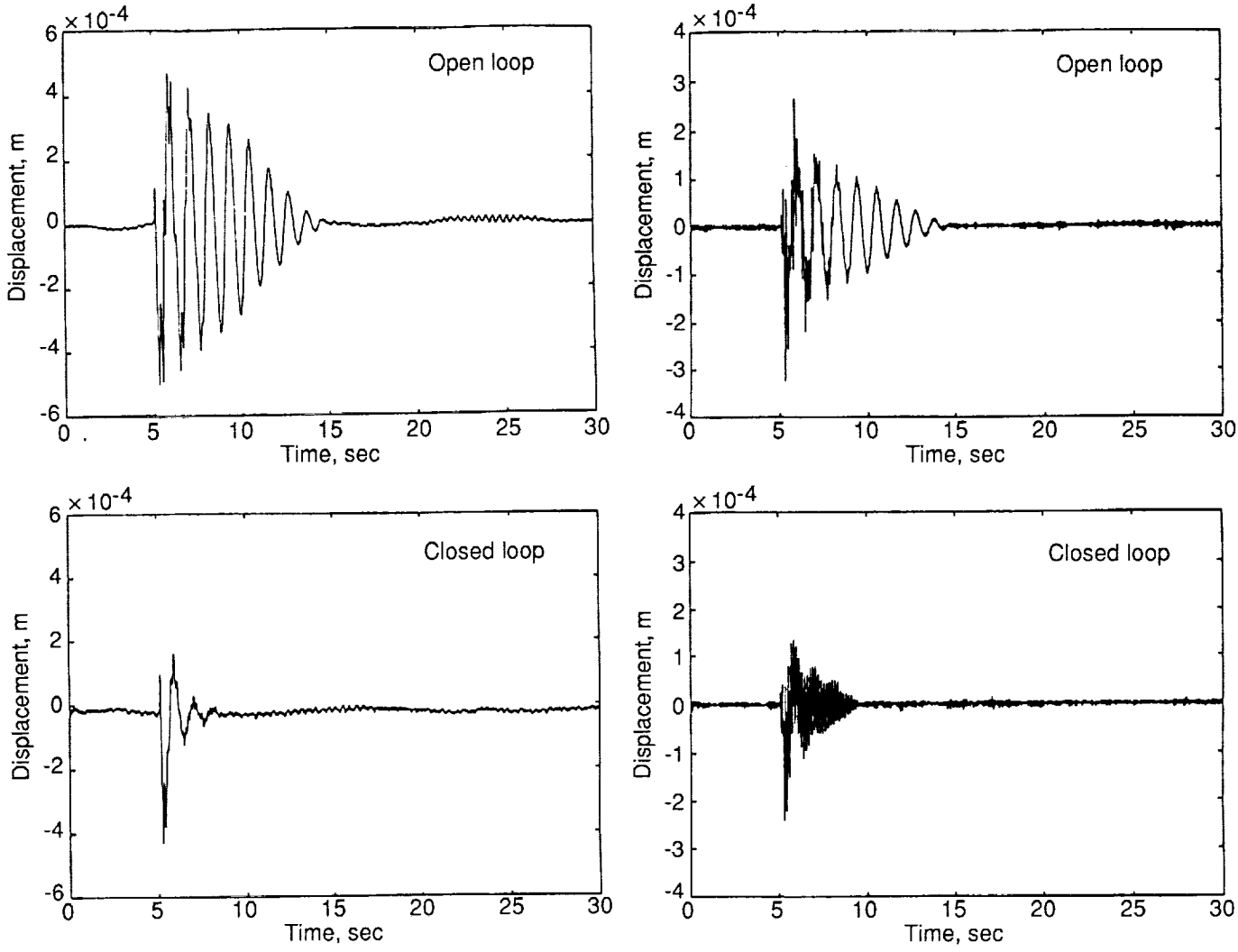

(a) Bay 18 responses.

(b) Bay 10 responses.

Figure 15. Mini-MAST displacement sensor responses for open loop and closed loop with MIMO positivity controller.

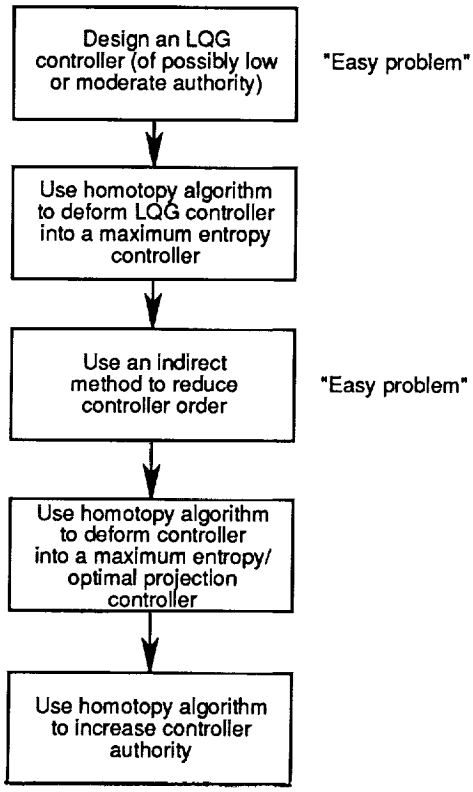

Figure 16. Maximum entropy/optimal projection control design process.

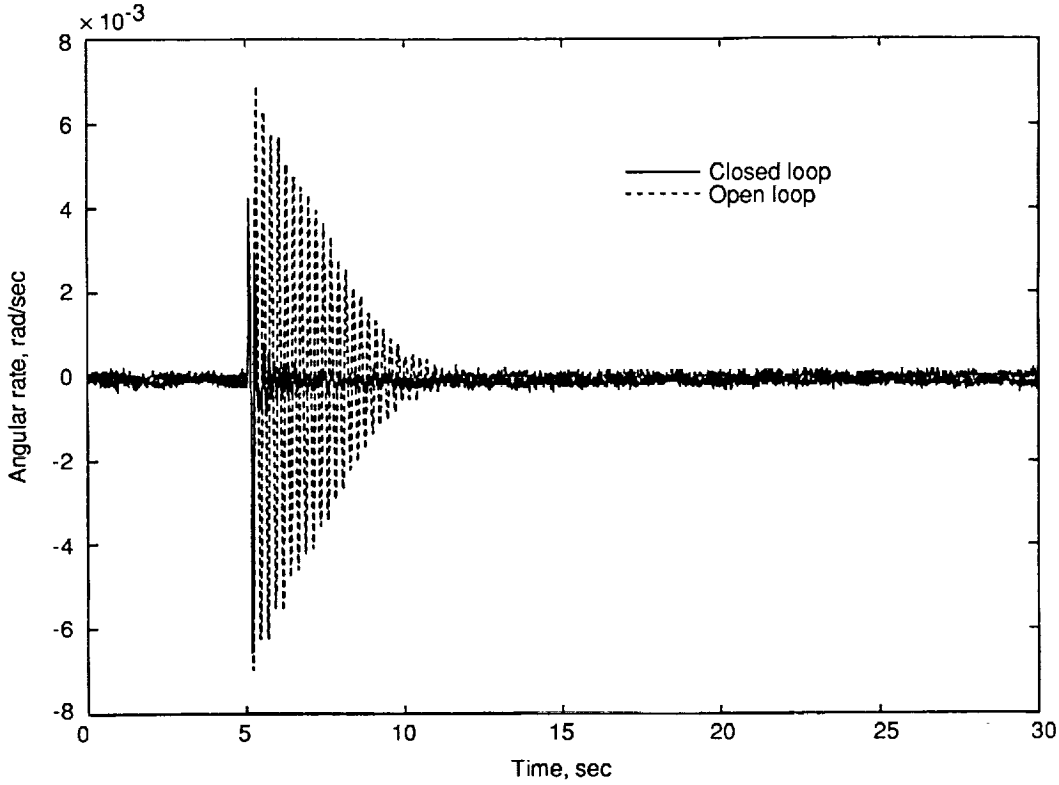

Figure 17. Open-loop versus closed-loop rate gyro-Z response for constant-gain feedback from gyro-Z to torque-Z.

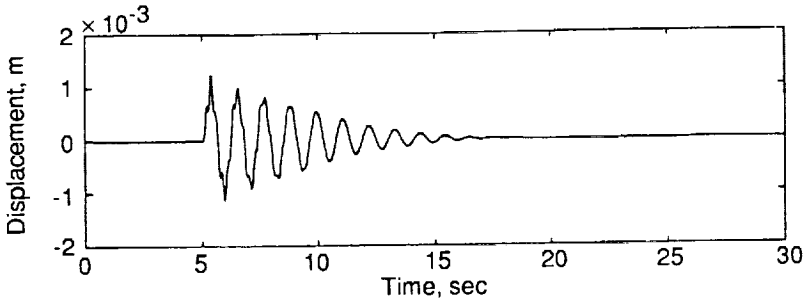

(a) Open-loop response.

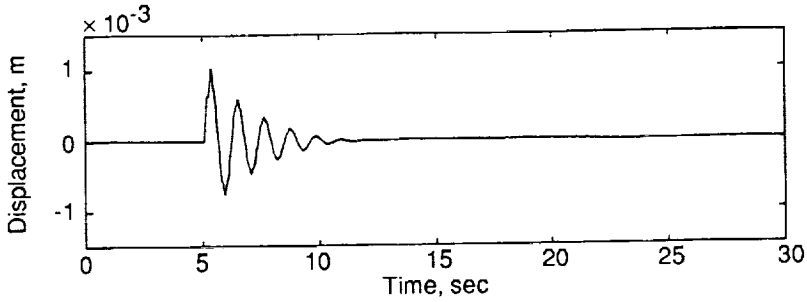

(b) Closed-loop response; pseudo-rate feedback.

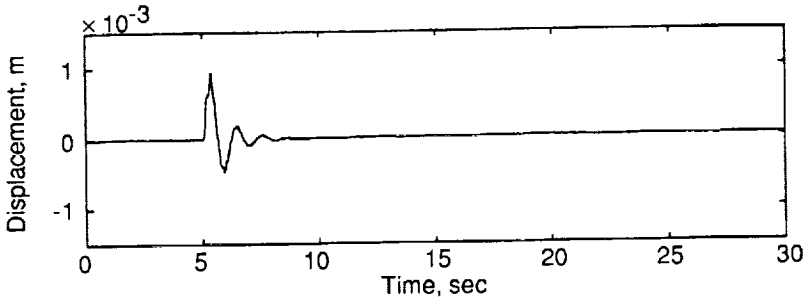

(c) Closed-loop response; "best" decentralized (24th order).

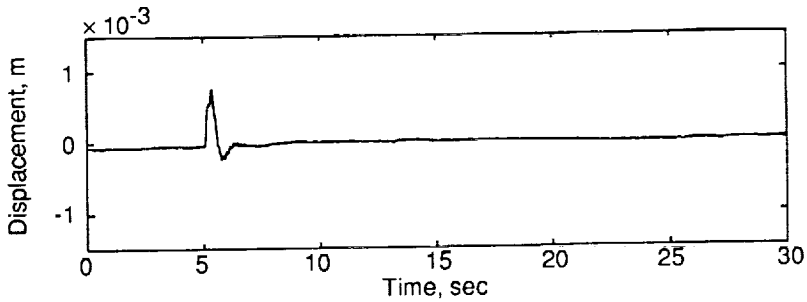

(d) Closed-loop response; "best" centralized (33rd order).

Figure 18. Mini-MAST controller series—open- and closed-loop responses of displacement A of bay 18.

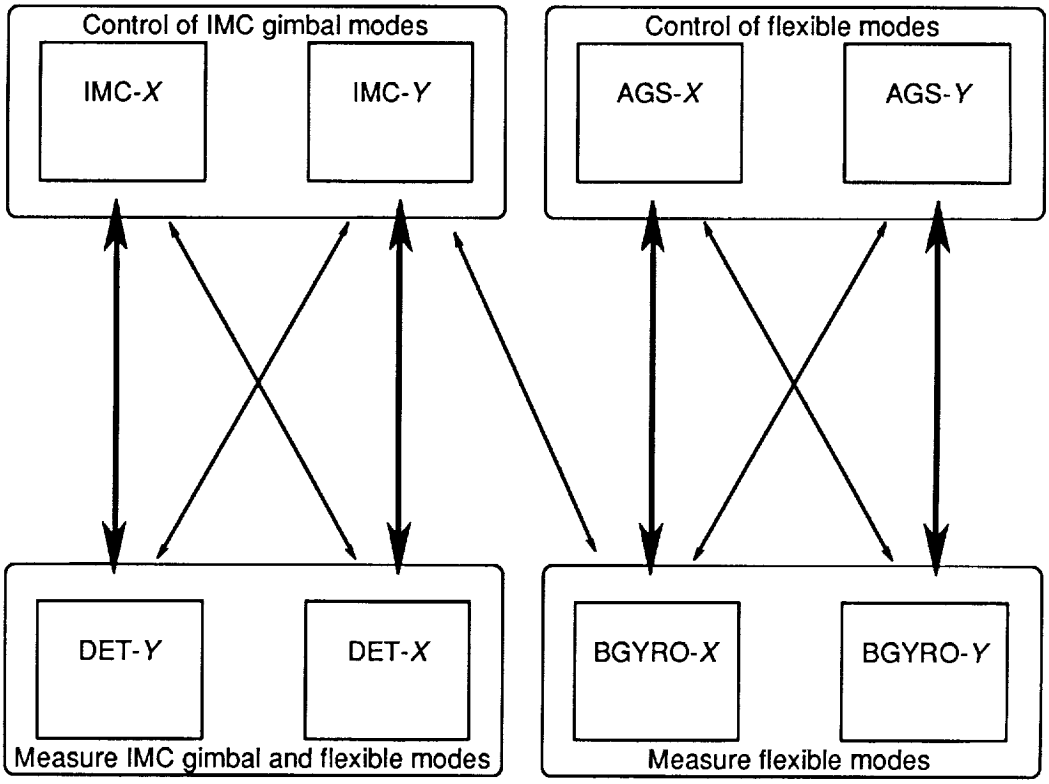

Figure 19. ACES dominant transfer function loops.

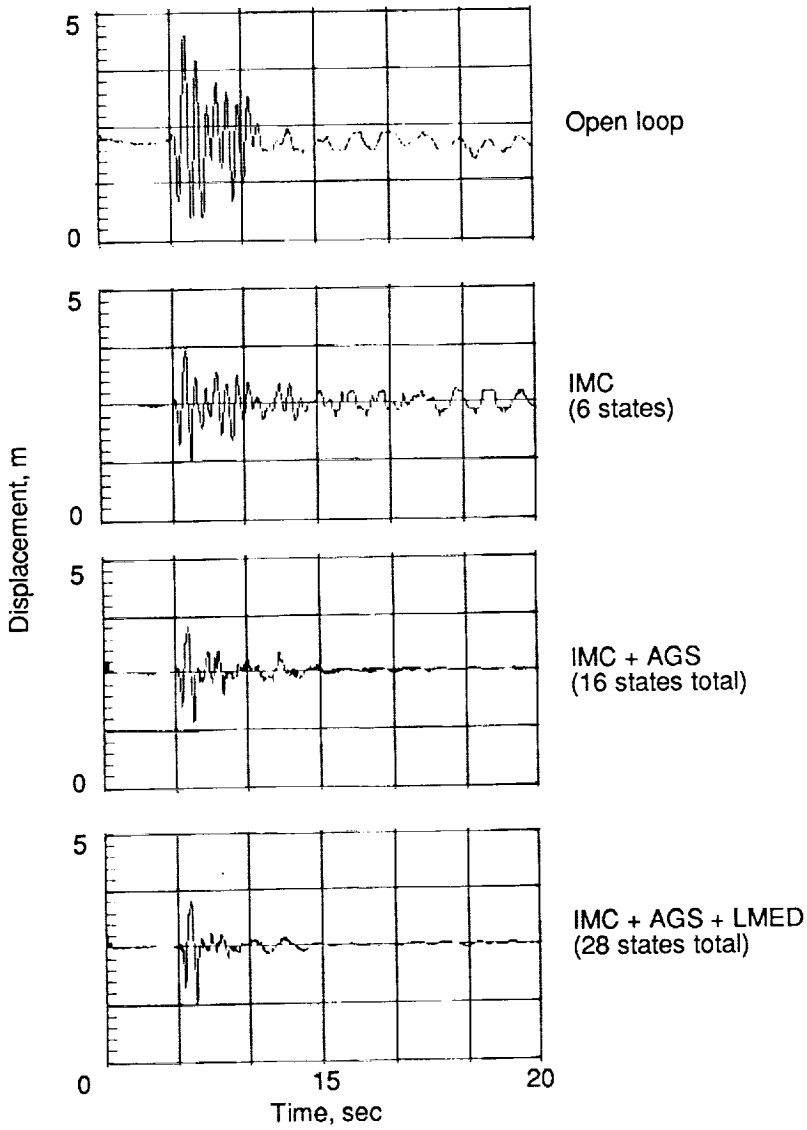

Figure 20. ACES results for integrated controller series.

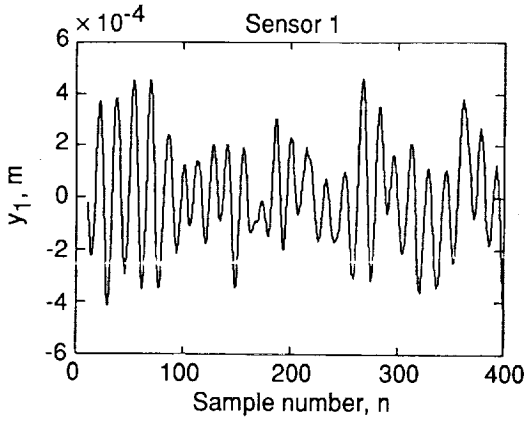

(a) Sensor output.

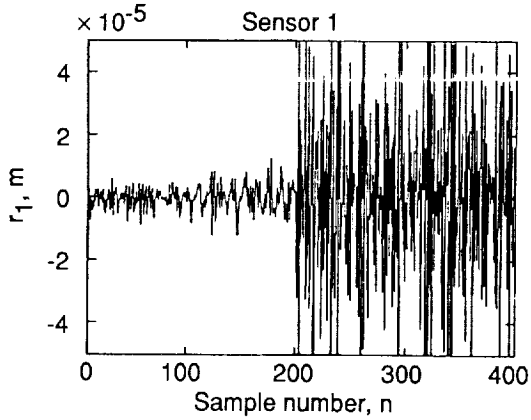

(b) SSPR residual output.

Figure 21. Displacement sensor with added noise failure mode.

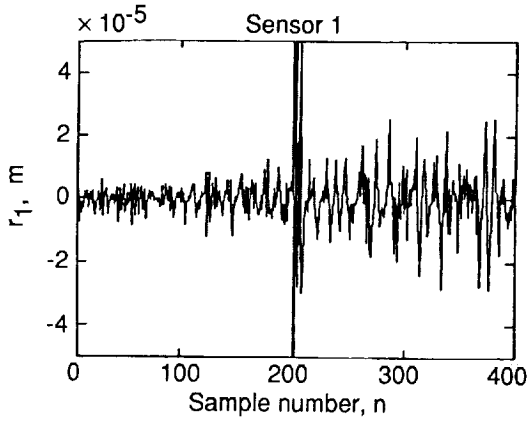

(a) SSPR residual reading (r_1).

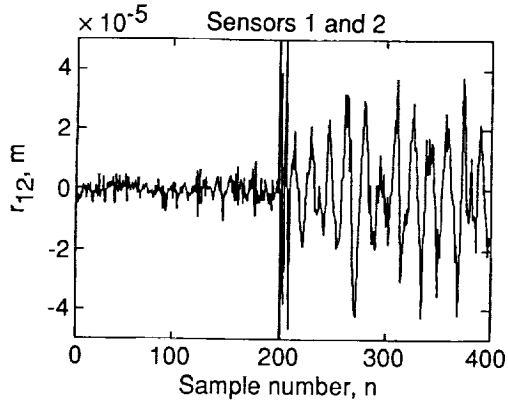

(b) DSPR residual reading (r_{12}).

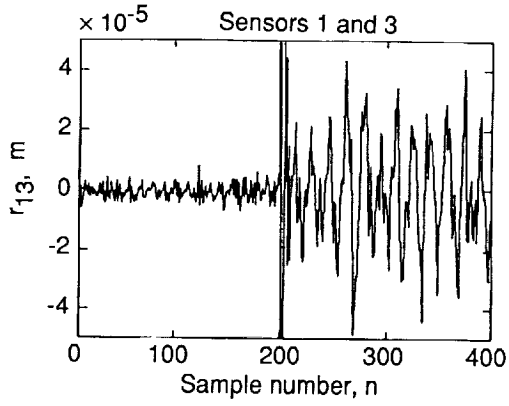

(c) DSPR residual reading (r_{13}).

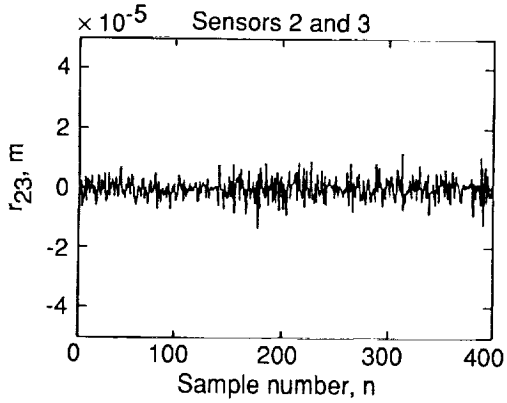

(d) DSPR residual reading (r_{23}).

Figure 22. Displacement sensor residuals with off failure mode.

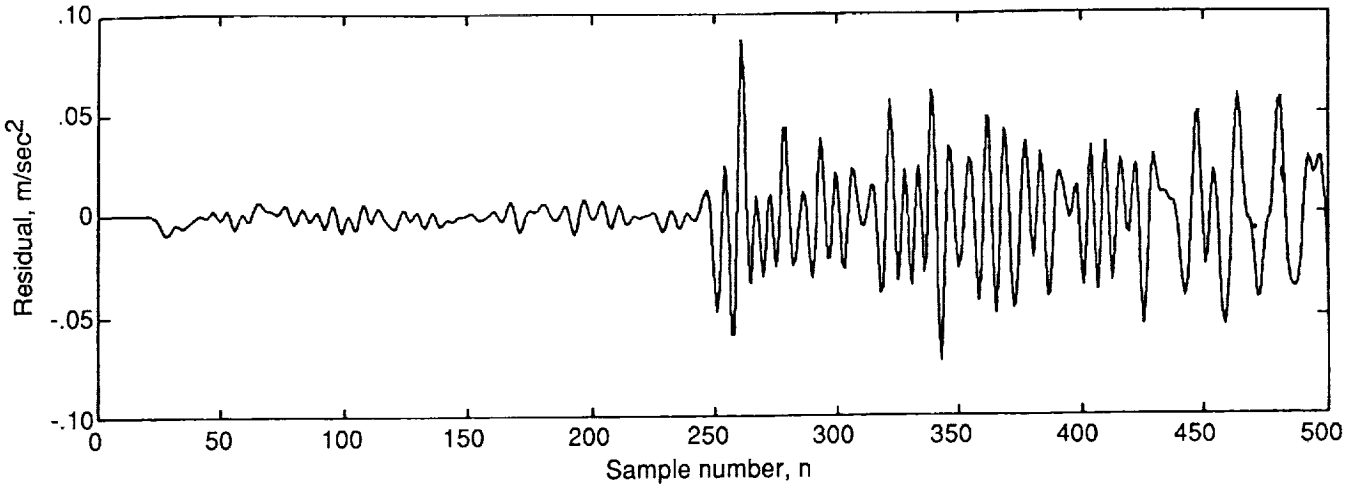

(a) Two accelerometers.

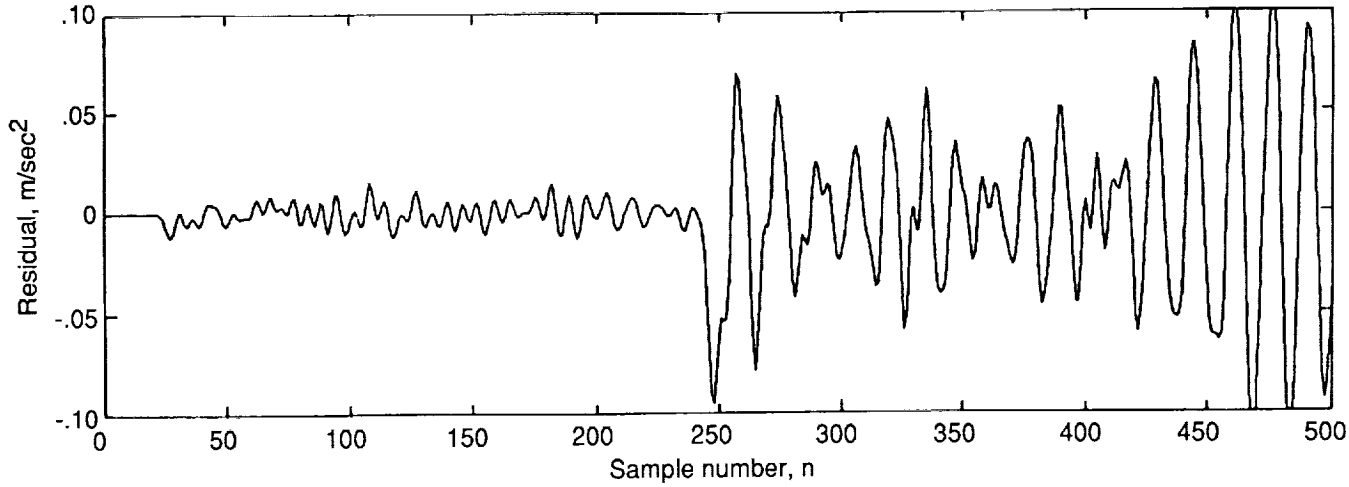

(b) Accelerometer and rate gyro.

Figure 23. Residuals for filtered double-sensor parity relation.

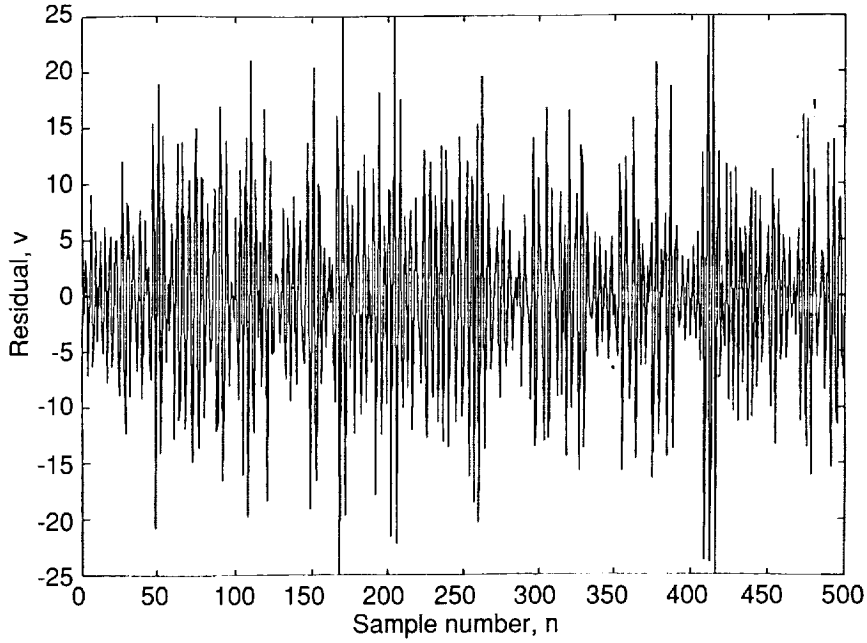

(a) SAPR for actuator failure at sample number 250.

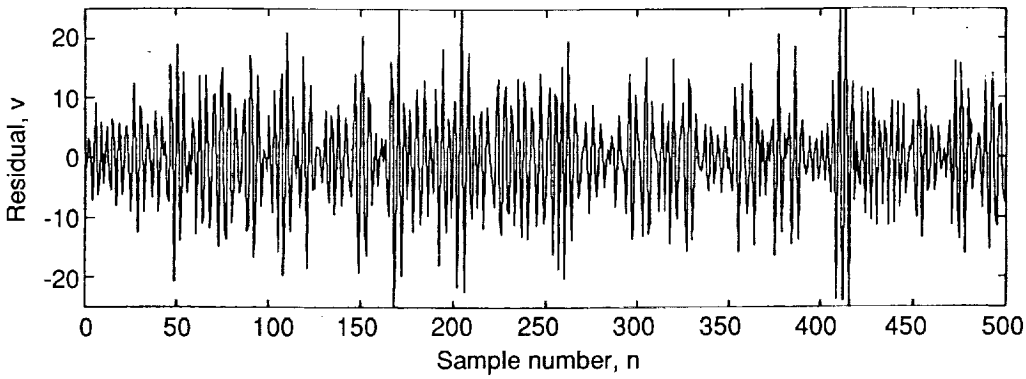

(b) Portion of SAPR attributable to nonfailed sensors.

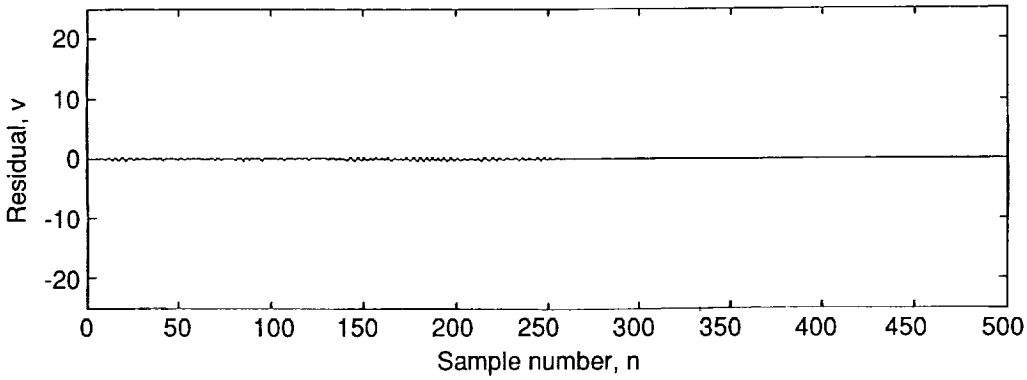

(c) Portion of SAPR attributable to residual for failed actuator.

Figure 24. SAPR for Mini-MAST actuator failure.

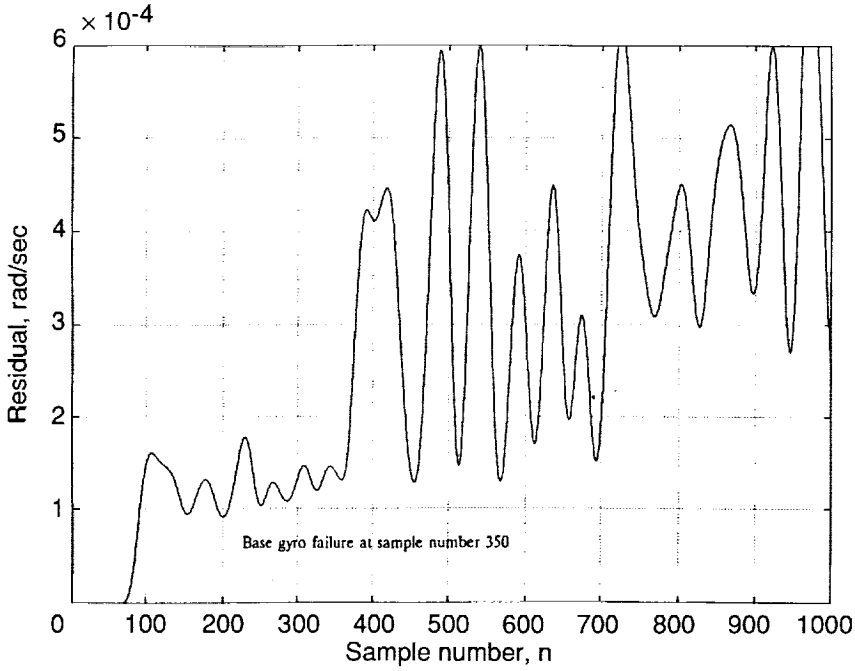

(a) DSPR using two rate gyros.

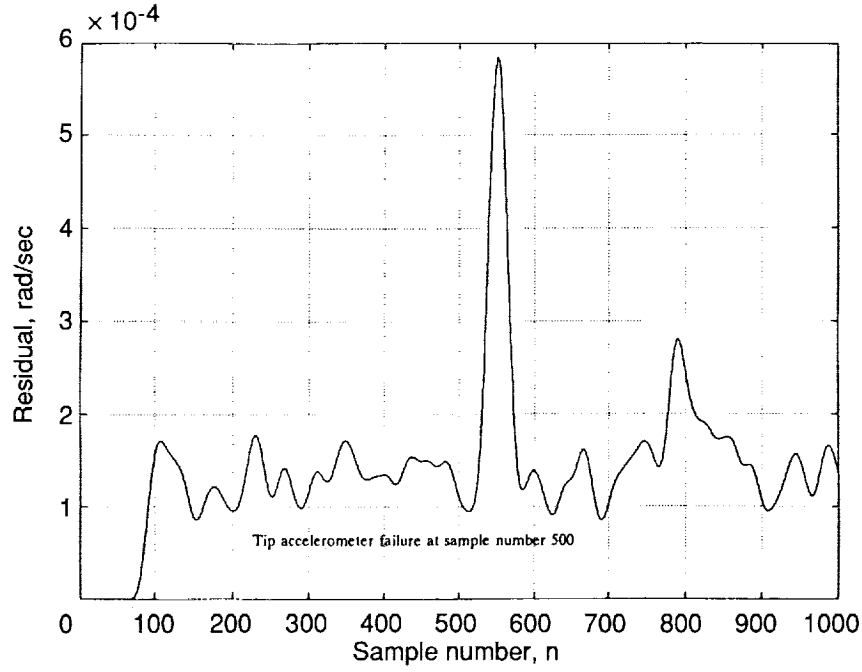

(b) DSPR using rate gyro and accelerometer.

Figure 25. ACES DSPR signatures.

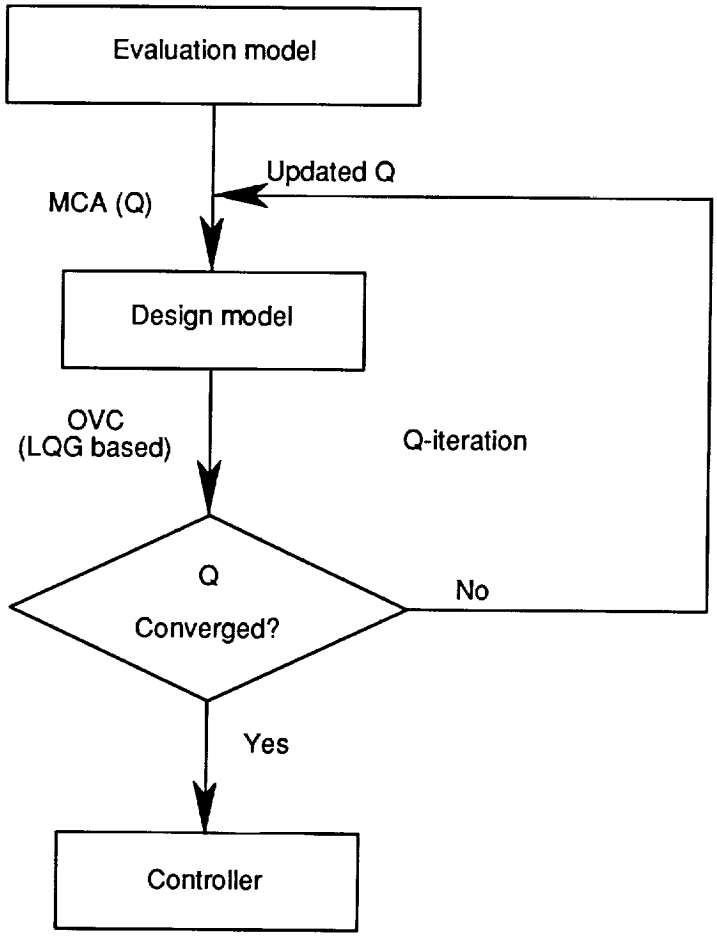

Figure 26. Integration of MCA modeling and OVC controller design.

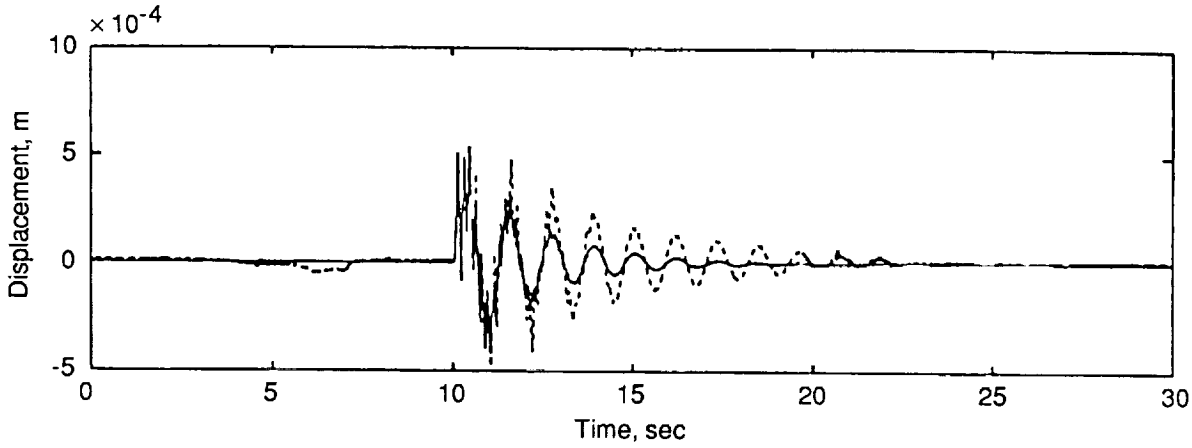

Figure 27. Displacement sensor response at Mini-MAST mid plate. Solid line indicates closed loop; dashed line indicates open loop.

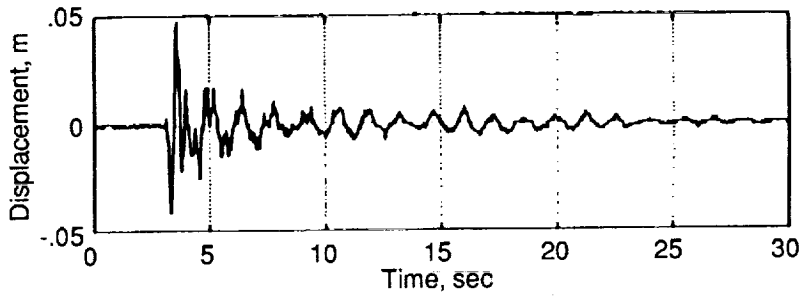

(a) Open-loop response.

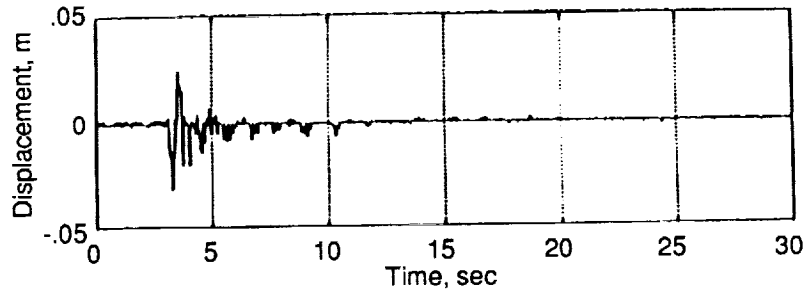

(b) Closed-loop response.

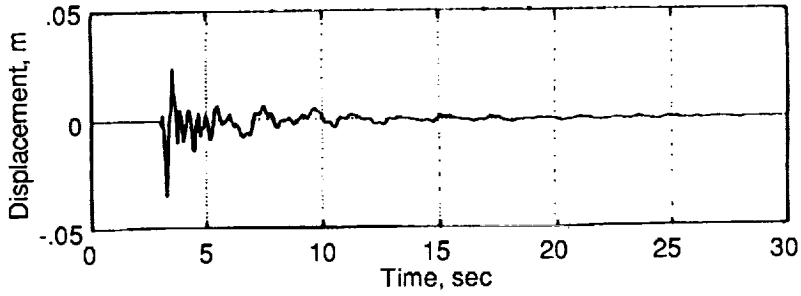

(c) Simulated closed-loop response.

Figure 28. ACES results with a 44th-order OVC controller.

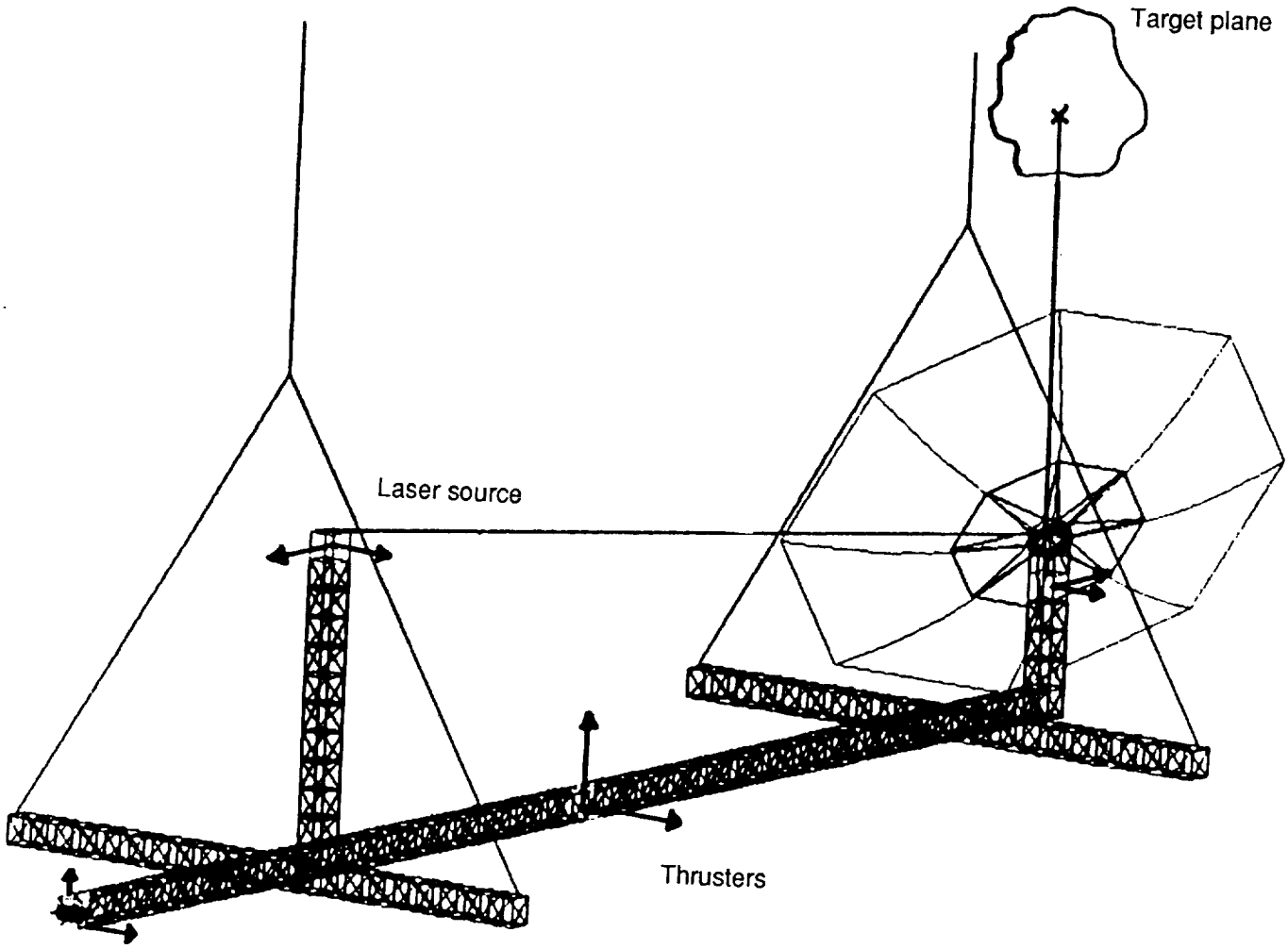

Figure 29. CSI evolutionary model schematic.

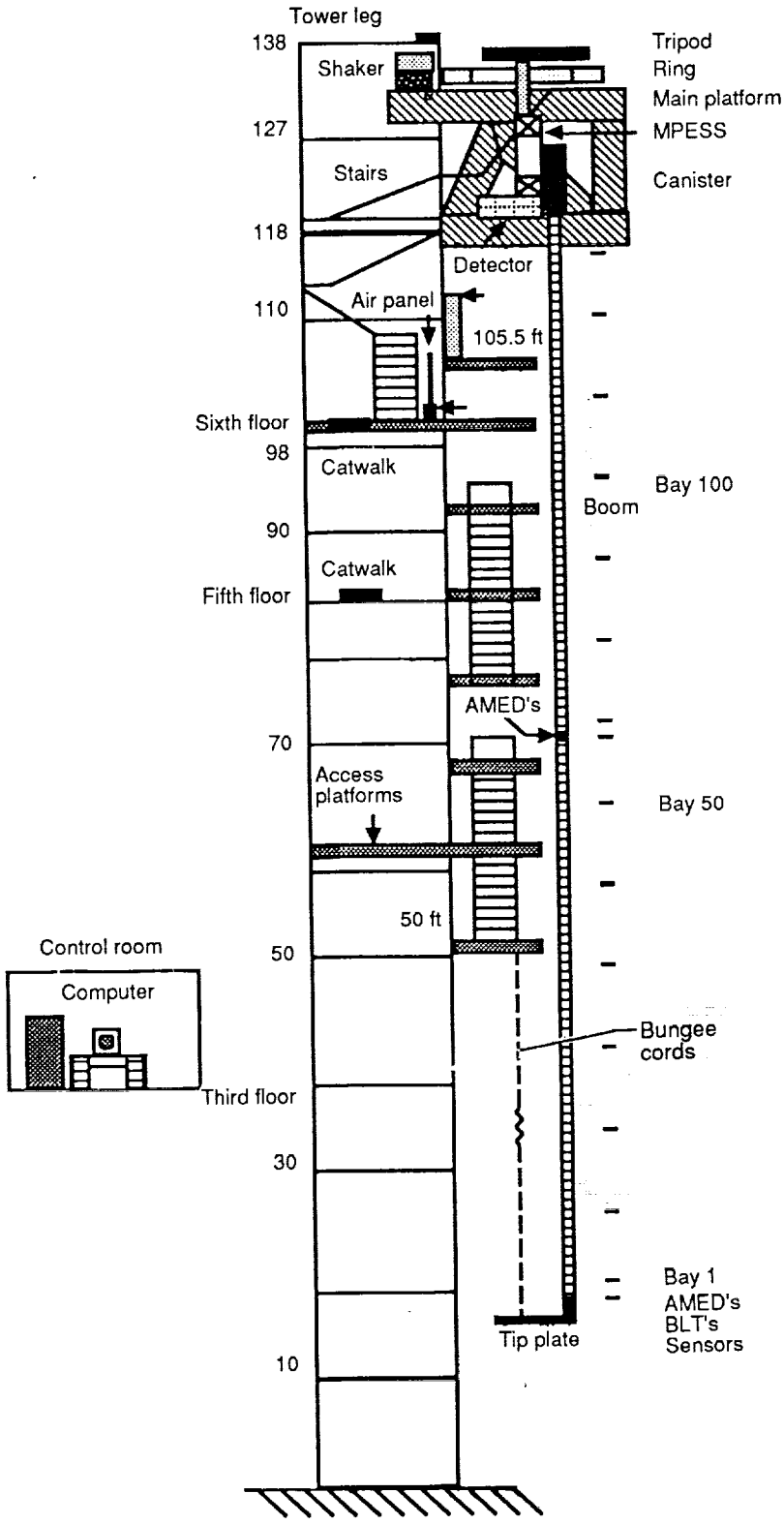

Figure 30. CASES ground test facility. Dimensions are in feet.

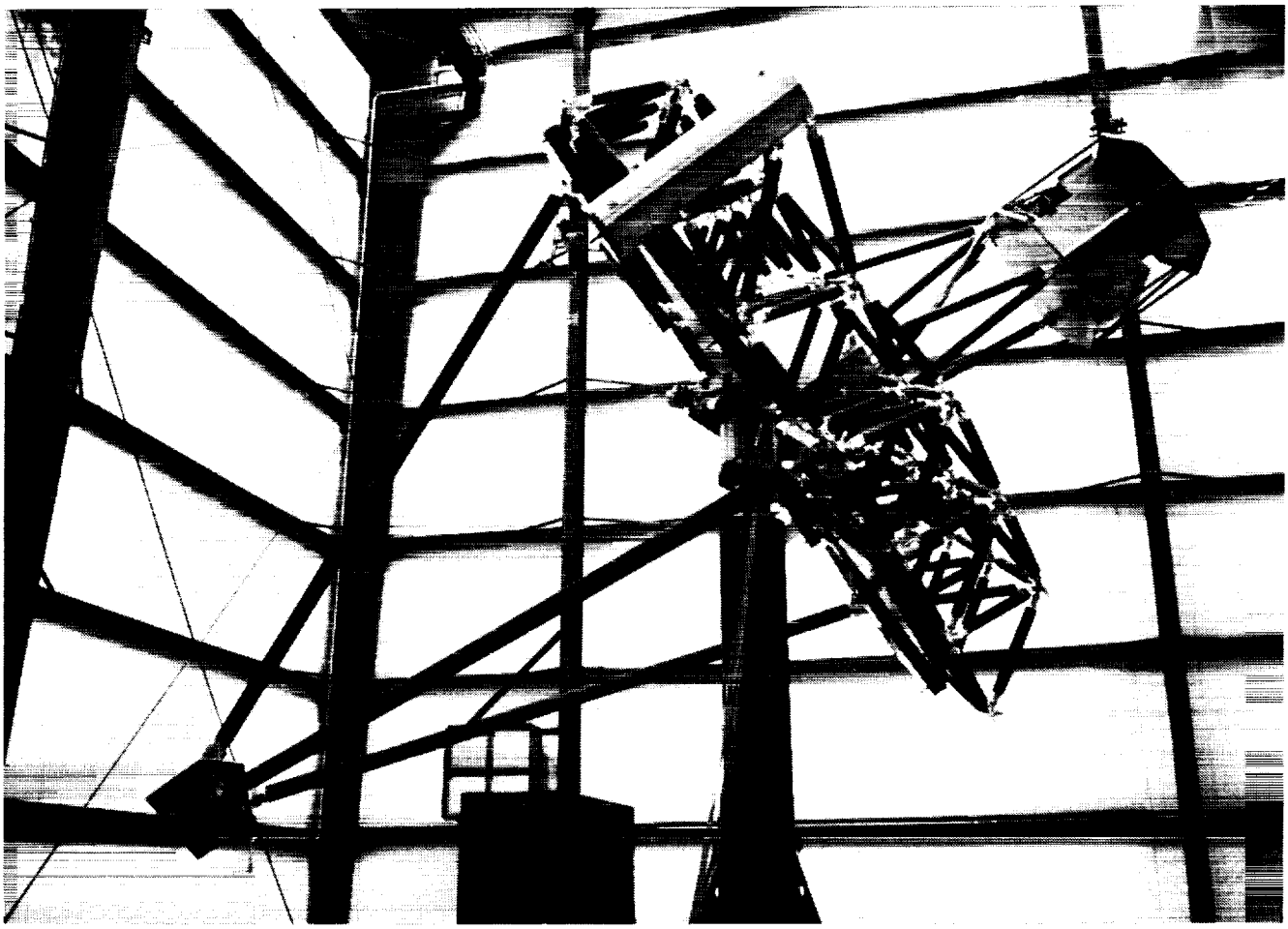

L-91-4187

Figure 31. ASTREX photograph.

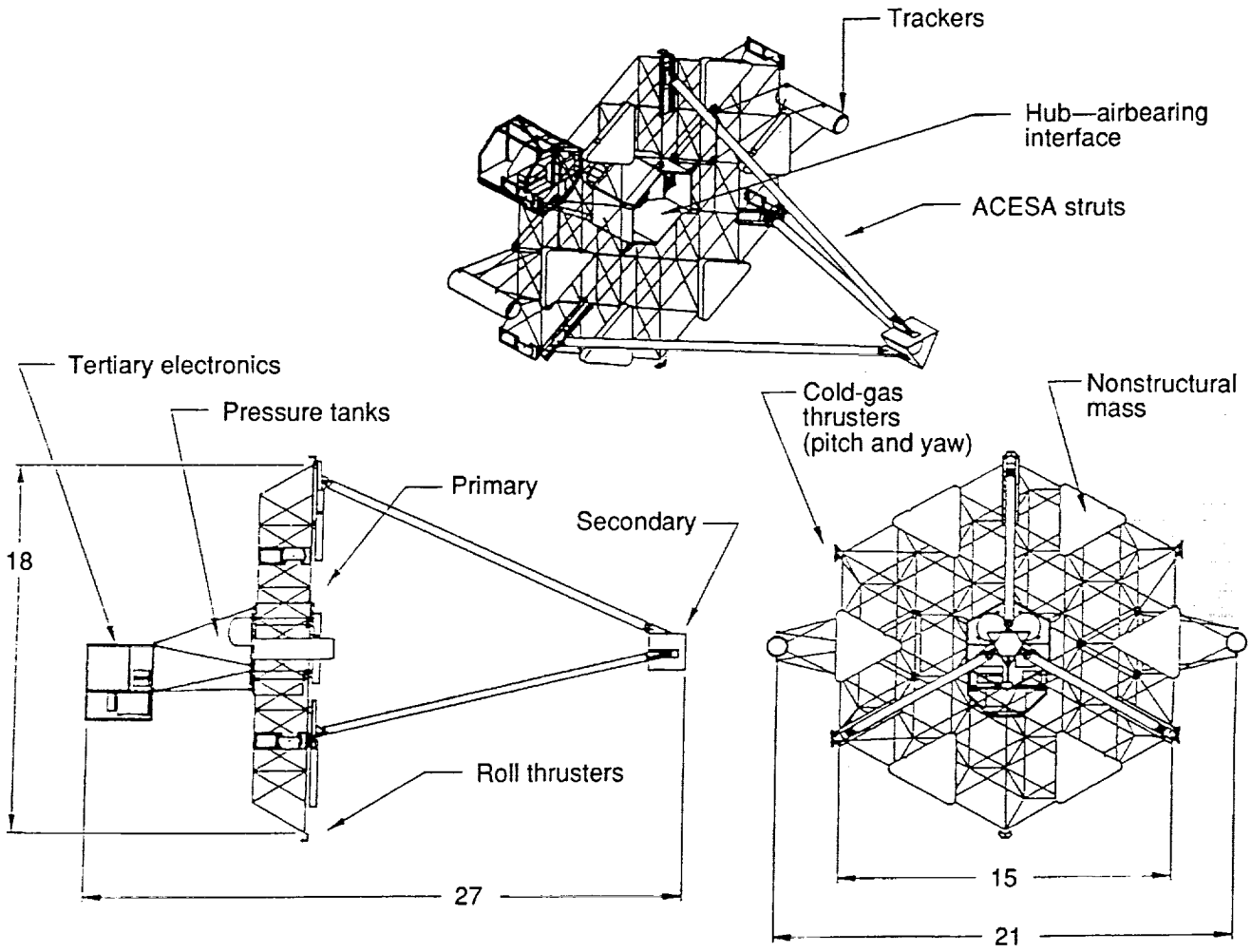

Figure 32. ASTREX schematic. Dimensions are in feet.

REPORT DOCUMENTATION PAGE

Form Approved
OMB No. 0704-0188

1. AGENCY USE ONLY *(Leave blank)*	2. REPORT DATE	3. REPORT TYPE AND DATES COVERED
	February 1993	Technical Memorandum

4. TITLE AND SUBTITLE
Controls-Structures Interaction Guest Investigator Program
Overview and Phase I Experimental Results and Future Plans

5. FUNDING NUMBERS
WU 590-14-91-01

6. AUTHOR(S)
Rudeen Smith-Taylor and Sharon E. Tanner

7. PERFORMING ORGANIZATION NAME(S) AND ADDRESS(ES)
NASA Langley Research Center
Hampton, VA 23681-0001

8. PERFORMING ORGANIZATION REPORT NUMBER
L-17052

9. SPONSORING/MONITORING AGENCY NAME(S) AND ADDRESS(ES)
National Aeronautics and Space Administration
Washington, DC 20546-0001

10. SPONSORING/MONITORING AGENCY REPORT NUMBER
NASA TM-4412

11. SUPPLEMENTARY NOTES
Presented at the American Astronautical Society Guidance and Control Conference, Keystone, Colorado, February 2 6, 1991.
A93-15590

12a. DISTRIBUTION/AVAILABILITY STATEMENT
Unclassified Unlimited

Subject Category 18

12b. DISTRIBUTION CODE

13. ABSTRACT *(Maximum 200 words)*

The integration of the design of control systems with the structural dynamics of flexible spacecraft can significantly benefit spacecraft performance but requires a multidisciplinary approach to the design process. Such an approach is being taken by the NASA Controls-Structures Interaction (CSI) Program, whose objective is to develop and validate the technology needed for the structure and the control system to interact beneficially to meet the requirements of future space missions. The CSI guest investigator (GI) program provides researchers the use of government testbeds to validate advanced control techniques and integrated designs. The objective of the GI program is to support CSI technology advancement by (1) involving researchers from academia and industry, (2) providing advanced CSI test facilities for experimental validation, and (3) disseminating the experimental results to the research community in a timely manner. Phase I of the GI program was initiated in 1988, with the selection of eight CSI researchers from industry and academia, to conduct research in two government test facilities. The report contains a program review of the 2-year activity, a description of the test facilities, and a summary of the experimental results. The report also briefly discusses the joint NASA-Air Force phase II program, the guest investigators selected, and the new testbeds they will use.

14. SUBJECT TERMS	15. NUMBER OF PAGES
Controls-structures interaction; Ground-based experiments; Guest investigator program; Active control techniques	47
	16. PRICE CODE A03

17. SECURITY CLASSIFICATION OF REPORT	18. SECURITY CLASSIFICATION OF THIS PAGE	19. SECURITY CLASSIFICATION OF ABSTRACT	20. LIMITATION OF ABSTRACT
Unclassified	Unclassified		